in the H12-PEG-polyAlb was acceptable for the in vivo study.

The PEG-polyAlb tended to prolong the blood circulation time of the particles with increasing modification amount of mPEG (Fig. 1). Especially, in the case of maximum mPEG modification, the amount of FITC-labeled PEG-polyAlb at a dose of 40 mg per kg gradually decreased to 91, 89, 75, 58, 57, and 54 percent after 10, 15, 30, 60, 120, and 180 minutes, respectively (taken as 100% just after injection). Consequently, we confirmed that the $t_{1/2}$ of the PEG-polyAlb was approximately 20-fold longer than that of the bare polyAlb due to the effect of PEG modification, suggesting that the PEG-polyAlb was likely to be useful for prophylactic transfusion. Sou and coworkers[38] previously reported the circulation kinetics of phospholipid vesicles at a dose of 14 mL per kg when infused into rats and rabbits. The $t_{1/2}$ of the vesicles in rabbits was approximately twofold longer than that in rats and estimated to be equal to that in humans. This inference was based on the biodistribution of the injected particles into various organs in which the balance between organ weight and body weight is a fundamental factor determining the pharmacokinetics of the vesicles.[38] We expected that the absolute $t_{1/2}$ of the H12-PEG-polyAlb in humans was estimated to be 6 hours, and the particles may be useful as prophylactic transfusions. We are now studying the $t_{1/2}$ and hemostatic effects of the H12-PEG-polyAlb using rabbits with severe thrombocytopenia.

It is possible that the excluded volume effect of the neighboring PEG chains could shield the recognition site of H12. Therefore, we used flow cytometry to determine whether the H12-PEG-polyAlb maintained the binding ability toward thrombin-stimulated PLTs even if the polyAlb was modified with PEG chains. We found that the H12-PEG-polyAlb bound extensively to the thrombin-stimulated PLTs, whereas it did not bind to resting PLT as well as the H12-polyAlb[31] (Fig. 2). From a viewpoint of side effects, it is very important for the H12-PEG-polyAlb to interact with only the activated PLTs and not to interact with resting PLTs because of acceleration of pathologic thrombosis in the bloodstream. The binding of the H12-PEG-polyAlb to the stimulated PLTs was significantly inhibited by PAC-1, indicating that the H12-PEG-polyAlb specifically bound to the activated GPIIb/IIIa on the surface of the PLTs via H12 conjugated to the end of the PEG chain. Furthermore, we confirmed that the binding ability of the H12-PEG-polyAlb was equal to that of the H12-polyAlb.[31] It was therefore expected that H12-PEG-polyAlb may also have a hemostatic effect as well as H12-polyAlb after PEG modification.

Finally, we evaluated the hemostatic property of the H12-PEG-polyAlb with thrombocytopenic rats. In our previous studies, we succeeded in preparing thrombocytopenic rats by busulfan administration and obtaining the extinction curve of PLTs reproducibly.[31] Using hematologic indices, we determined that the concentration of busulfan, at which the PLT counts were sufficiently decreased and the RBC and white blood cell counts were maintained, was 20 mg per kg for 8-week-old rats. We further determined that the best day for the incision of the tail was Day 10 after busulfan infusion. From our previous study, the bleeding time was confirmed to correlate with PLT counts of the rats.[31]

We confirmed the dose-dependent nature of the hemostatic effect of the H12-PEG-polyAlb in vivo with moderately thrombocytopenic rats at 3 hours after infusion of the particles, suggesting that the polyAlb may be a promising candidate for a PLT substitute (Fig. 3). Based on our previous studies of latex beads carrying H12 and analyses of PLT aggregation under flow conditions with a scanning electron microscope,[30] we considered that the enhancing mechanism of H12-PEG-polyAlb was similar to that of the latex beads carrying H12 for the following reasons: 1) the adhesion of the H12-PEG-polyAlb could be initiated by the activated PLTs, which had already adhered on the surface of the exposed collagen at the vascular injury; 2) the H12-PEG-polyAlb adhering to the surface of the PLT could act as binding sites for the activated PLTs; and 3) the H12-PEG-polyAlb could accelerate the formation of the thrombus of the flowing PLTs in the thrombocytopenic blood. In contrast, the H12-polyAlb (not modified with PEG), which had a measurable hemostatic effect at 5 minutes after IV administration in our previous study,[31] did not reduce the bleeding time at 3 hours. Furthermore, we estimated the hemostatic capacity of the H12-PEG-polyAlb in comparison with PLT based on particle number. The particle number of the H12-PEG-polyAlb at a dose of 40 mg per kg was estimated to approximately 900×10^9 particles at 3 hours after IV administration. The bleeding time of the H12-PEG-polyAlb (330 ± 73 sec) was similar to that of the rats at a PLT number of approximately 10×10^9, based on the relationship between the bleeding time of the thrombocytopenic rats and PLT count.[31] This indicated that the H12-PEG-polyAlb was easy to adhere to the activated PLTs and aggregate with the PLTs on the vascular injury because the amount of H12 conjugated to the surface of polyAlb was relatively abundant. Furthermore, we also confirmed that hematologic indices did not change before and after the infusion of the H12-PEG-polyAlb. Furthermore, we confirmed that the hemostatic effect of the H12-PEG-polyAlb at a dose of 40 mg per kg lasted for at least 6 hours; however, at 12 hours after infusion, the tail bleeding time was comparable to that of the saline group, suggesting that the tail bleeding time correlated with the $t_{1/2}$ of H12-PEG-polyAlb and that the circulating H12-PEG-polyAlb may remain hardly in the bloodstream at 12 hours.

In conclusion, we succeeded in prolongation of the in vivo $t_{1/2}$ of H12-conjugated polyAlb by PEG modification (H12-PEG-polyAlb) and confirmed that the H12-PEG-polyAlb maintained specific binding ability to activated PLTs. Furthermore, the H12-PEG-polyAlb dose dependently shortened the tail bleeding time of thrombocytopenic rats and the hemostatic effects lasted for at least 6 hours. Thus, the H12-PEG-polyAlb may be a suitable candidate for an alternative to human PLT concentrates infused into thrombocytopenic patients for the treatment of bleeding. In our future prospects, we are planning to assess the hemostatic ability of the H12-PEG-polyAlb during surgery on the animals with severe thrombocytopenia and to study the safety of the H12-PEG-polyAlb as PLT substitutes with normal animals and rabbits with hereditary hyperlipidemia, which are so-called Watanabe rabbits, whether the particles will accelerate pathologic thrombosis, and whether the particles will accelerate or inhibit fibrinolysis.

ACKNOWLEDGMENTS

The authors thank M. Murata, MD, PhD, and K. Yokoyama, MD, PhD, at Keio University for useful discussion about the functional evaluation of H12 peptide.

REFERENCES

1. Blajchman MA. Substitutes and alternatives to platelet transfusions in thrombocytopenic patients. J Thromb Haemost 2003;1:1637-41.
2. Graham SS, Gonchoroff NJ, Miller JL. Infusible platelet membranes retain partial functionality of the platelet GPIb/IX/V receptor complex. Am J Clin Pathol 2001;115: 144-7.
3. Rybak M, Renzulli LA. A liposome based platelet substitute, the plateletsome, with hemostatic efficacy. Biomater Artif Cells Immobilization Biotechnol 1993;21:108-18.
4. Agam G, Livine AA. Erythrocytes with covalently bound fibrinogen as a cellular replacement for the treatment of thrombocytopenia. Eur J Clin Invest 1992;22:105-12.
5. Levi M, Friedrich PW, Middleton S, et al. Fibrinogen-coated albumin microcapsules reduce bleeding in severely thrombocytopenic rabbits. Nat Med 1999;5:107-11.
6. Casals E, Verdaguer A, Tonda R, et al. Atomic force microscopy of liposomes bearing fibrinogen. Bioconjugate Chem 2003;14:593-600.
7. Coller BS, Springer KT, Beer JH, et al. Thromboerythrocytes: in vitro studies of a potential autologous, semi-artificial alternative to platelet transfusion. J Clin Invest 1992;89: 546-55.
8. Takagi J, Petre BM, Walz T, Springer TA. Global comformational rearrangements in integrin extracellular domains in outside-in and inside-out signaling. Cell 2002;110:599-611.
9. Xiao T, Takagi J, Coller BS, Wang JH, Springer TA. Structural basis for allostery in integrins and binding to fibrinogen-mimetic therapeutics. Nature 2004;432:59-67.
10. Shattil SJ, Hoxie JA, Cunningham M, Brass LF. Changes in the platelet membrane glycoprotein IIb-IIIa complex during platelet activation. J Biol Chem 1985;260:11107-14.
11. Marguerie GA, Plow EF, Edgington TS. Human platelets possess an inducible and saturable receptor specific for fibrinogen. J Biol Chem 1979;254:5357-63.
12. Ruggeri ZM, De Marco L, Gatti L. Platelets have more than one binding site for von Willebrand factor. J Clin Invest 1983;72:1-12.
13. Mustard JF, Packham MA, Kinlough-Rathbone RL. Fibrinogen and ADP-induced platelet aggregation. Blood 1978;52: 453-66.
14. De Marco L, Girolami A, Zimmerman TS. Von Willebrand factor interaction with the glycoprotein IIb/IIIa complex. J Clin Invest 1986;77:1272-7.
15. Hawiger J, Kloczewiak M, Bednarek MA, Timmons S. Platelet receptor recognition domains on the α chain of human fibrinogen: structure-function analysis. Biochemistry 1989; 28:2909-14.
16. Kloczewiak M, Timmons S, Hawiger J. Localization of a site interacting with human platelet receptor on carboxy-terminal segment of human fibrinogen γ chain. Chain Biochem Biophys Res Commun 1982;107:181-7.
17. Takeoka S, Teramura Y, Okamura Y, et al. Fibrinogen-conjugated albumin polymers and their interaction with platelets under flow conditions. Biomacromolecules 2001; 2:1192-7.
18. Takeoka S, Teramura Y, Ohkawa H, Ikeda Y, Tsuchida E. Conjugation of von Willebrand factor-binding domain of platelet glycoprotein Ibα to size-controlled albumin microsheres. Biomacromolecules 2000;1:290-5.
19. Teramura Y, Okamura Y, Takeoka S, et al. Hemostatic effects of polymerized albumin particles bearing rGPIa/IIa in thrombocytopenic mice. Biochem Biophys Res Commun 2003;306:256-60.
20. Takeoka S, Teramura Y, Okamura Y, et al. Rolling properties of rGPIbα-conjugated phospholipid vesicles with different membrane flexibilities on vWf surface under flow conditions. Biochem Biophys Res Commun 2002;296:765-70.
21. Kitaguchi T, Murata M, Iijima K, et al. Characterization of liposomes carrying von Willebrand factor-binding domain of platelet glycoprotein Ibα: a potential substitute for platelet transfusion. Biochem Biophys Res Commun 1999; 261:784-9.
22. Nishiya T, Murata M, Handa M, Ikeda Y. Targeting of liposomes carrying recombinant fragments of platelet membrane glycoprotein Ibα to immobilized von Willebrand factor under flow conditions. Biochem Biophys Res Commun 2000;270:755-60.
23. Nishiya T, Kainoh M, Murata M, Handa M, Ikeda Y. Reconstitution of adhesive properties of human platelets in

liposomes carrying both recombinant glycoproteins Ia/IIa and Ibα under flow conditions: specific synergy of receptor–ligand interactions. Blood 2002;100:136-42.
24. Okamura Y, Maekawa Y, Teramura Y, et al. Hemostatic effects of phospholipid vesicles carrying fibrinogen γ-chain dodecapeptide in vitro and in vivo. Bioconjugate Chem 2005;16:1589-96.
25. Wertheimer E, Shapiro B, Fodor-Salomonowicz I. Stability of fibrinogen in normal and pathological plasma. Br J Exp Pathol 1944;25:121-5.
26. Kloczewiak M, Timmons S, Lukas TJ, Hawiger J. Platelet receptor recognition site on human fibrinogen. Synthesis and structure-function relationship of peptides corresponding to the carboxy-terminal segment of the γ chain. Biochemistry 1984;23:1767-74.
27. Kloczewiak M, Timmons S, Bednarek MA, Sakon M, Hawiger J. Platelet receptor recognition domain on the γ chain of human fibrinogen and its synthetic peptide analogues. Biochemistry 1989;28:2915-9.
28. Lam SC, Plow EF, Smith MA, et al. Evidence that arginyl-glycyl-aspartate peptides and γ chain peptides share a common binding site on platelets. J Biol Chem 1987;262:110-5.
29. Hallahan DE, Geng L, Cmelak AJ, et al. Targeting drug delivery to radiation-induced neoantigens in tumor microvasculature. J Control Release 2001;74:183-91.
30. Takeoka S, Okamura Y, Teramura Y, et al. Function of fibrinogen γ-chain dodecapeptide-conjugated latex beads under flow. Biochem Biophys Res Commun 2003;312:773-9.
31. Okamura Y, Takeoka S, Teramura Y, et al. Hemostatic effects of fibrinogen γ-chain dodecapeptide-conjugated polymerized albumin particles in vitro and in vivo. Transfusion 2005;45:1221-8.
32. Sakai H, Takeoka S, Park SI, et al. Surface modification of hemoglobin vesicles with poly(ethylene glycol) and effects on aggregation, viscosity, and blood flow during 90% exchange transfusion in anesthetized rats. Bioconjugate Chem 1997;8:23-30.
33. Sakai H, Tsai AG, Kerger H, et al. Subcutaneous microvascular responses to hemodilution with a red cell substitute consisting of polyethyleneglycol-modified vesicles encapsulating hemoglobin. J Biomed Mater Res 1998;40:66-78.
34. Klibanov AL, Maruyama K, Torchilin VP, Huang L. Amphipathic polyethyleneglycols effectively prolong the circulation time of liposomes. FEBS Lett 1990;268:235-7.
35. Zalipsky S. Functionalized poly(ethylene glycol) for preparation of biologically relevant conjugates. Bioconjugate Chem 1995;6:150-65.
36. Taub R, Gould RJ, Garsky VM, et al. A monoclonal antibody against the platelet fibrinogen receptor contains a sequence that mimics a receptor recognition domain in fibrinogen. J Biol Chem 1989;264:259-65.
37. Hristova K, Needham D. Phase behavior of a lipid/polymer-lipid mixture in aqueous medium. Macromolecules 1995;28:991-1002.
38. Sou K, Klipper R, Goins B, Tsuchida E, Phillips WT. Circulation kinetics and organ distribution of Hb-vesicles developed as a red blood cell substitute. J Phaemacol Exp Ther 2005;312:702-9.

DOI: 10.1002/adma.200700661

Ubiquitous Transference of a Free-Standing Polysaccharide Nanosheet with the Development of a Nano-Adhesive Plaster**

Toshinori Fujie, Yosuke Okamura, and *Shinji Takeoka**

Convenient fabrication or manipulation of nanoscale materials will significantly enhance the potential applicability of nanotechnology. One novel methodology for the fabrication of nanoscale materials involving a wide variety of macromolecules is the layer-by-layer (LbL) technique.[1] The LbL method involves alternative adsorption of oppositely charged polyelectrolytes by different non-covalent linking such as electrostatic interactions, hydrogen bonding, or hydrophobic interactions.[1a–d] Application of LbL-based materials has been explored in several fields, such as electrochemical devices, chemical sensors, nanomechanical sensors, nanoscale chemical/biological reactors, and as a drug-delivery system.[2] Nonetheless, potential applications of the LbL method ubiquitously apply to both the liquid and gas phases. Therefore, the ubiquitous manipulation of LbL-based nanocomposites is critical to the development of further functions in nanotechnology.

The LbL method has been applied to the construction of 3D nanocomposites, such as core/shell colloidal particles and hollow capsules.[3] The shells are composed of ultrathin multilayers built on a colloidal core. A hollow capsule is produced by removing the sacrificial template core. Recently, this sacrificial template idea has been applied to the film-fabrication process. Specifically, the LbL method has been used to fabricate a free-standing ultrathin membrane using a spin-coating-assisted LbL (SA-LbL) method.[4] The SA-LbL method can prepare ultrathin membranes by spin-coating each polyelectrolyte alternatively on a substrate covered with a sacrificial layer. Subsequent dissolution of the sacrificial layer releases the free-standing ultrathin membrane within several minutes, unlike conventional protocols that require many hours (e.g., a dipping LbL process). Because the membranes are composed of polymers with a sheetlike structure of nanometer thickness they possess a huge aspect ratio ($\geq 10^6$ depending on the size of the substrate). As such, these structures have been referred to as 'polymer nanosheets' by Miyashita.[5c] The free-standing polymer nanosheets released from the substrate were constructed not only by using the SA-LbL method, but also by using a Langmuir–Blodgett method crosslinking amphiphilic copolymers or by using a sol–gel method with organic–inorganic interpenetrating networks.[5] These polymer nanosheets bearing potential functions that are not available in bulk composites (such as high flexibility and transparency) nanocomposites have been reported to be well-organized, compliant, and robust materials for micro-/nanomechanical studies.[6] However, the polymer nanosheets do not maintain their shape after removal of the substrate and change from having a liquid phase to having a solid outer surface. This limitation is thought to be because the nanosheets with a huge aspect ratio are overwhelmed in the air.

In this communication, we focus on the convenient manipulation of the polymer nanosheet involving ubiquitous transfer from the liquid–solid surface to the air–solid surface using a water-soluble sacrificial membrane. This technique of transferring the polymer nanosheet will also explore the potential advantage of transferring the ultrathin films from the conventional solid substrate to any surfaces that are not always solid interface such as human skin or organs. Therefore, we applied this method to the construction of a new biomedical material called a 'nano-adhesive plaster', consisting of polysaccharides (i.e., a polysaccharide nanosheet) and demonstrated the release of the polysaccharide nanosheet into the human skin.

In order to fabricate the polysaccharide nanosheet, we used chitosan and sodium alginate (Na alginate), which have amino and carboxylic groups as cationic and anionic polyelectrolytes at ambient pH. These polysaccharides are used in biomedical fields as wound dressings and artificial skin because of their biocompatibility and biodegradability.[7] Furthermore, recent studies in LbL assembly using this biopolymer revealed the utility of polysaccharides for biomedical applications such as drug delivery and tissue engineering.[8] Therefore, we selected polysaccharides as the building blocks of the nanosheet. The methodology for the fabrication of the polysaccharide nanosheet utilizes the SA-LbL method as described in the Experimental section. Each polysaccharide was prepared in an aqueous solution containing 0.5 M NaCl in order to weaken the electrostatic interaction between the polyelectrolytes, thereby forming a smooth flat surface.[9] The nanosheet with 10.5 pairs of polysaccharide layers was prepared on a silicon wafer cov-

[*] Prof. S. Takeoka, T. Fujie, Dr. Y. Okamura
Department of Applied Chemistry
Graduate School of Science and Engineering
Waseda University
Tokyo, 169-8555 (Japan)
E-mail : takeoka@waseda.jp

[**] The authors thank Assoc. Prof. Dr. T. Shimamoto at the Consolidated Research Institute for Advanced Science and Medical Care, Waseda University for the technical advice and useful discussions about AFM measurements. This work was supported by the "Consolidated Research Institute for Advanced Science and Medical Care" from MEXT and the Shorai Foundation for Science and Technology (S.T.), Japan. T.F. was the scholar "Doctor-21" of the Yoshida Scholarship Foundation. Y.O. was the recipient of a Research Fellowship from the JSPS for Young Scientists.

ADVANCED MATERIALS

ered with an acetone-soluble photoresist sacrificial layer (OFPR-800 LB (200 cP); 2 μm thick, composed of a novolac resin and a photoactive compound). Upon fabrication of the polysaccharide nanosheet, the sacrificial layer was placed in acetone and the transparent nanosheet on the substrate was gradually detached from the edges of the substrate. After 20 min, the polysaccharide nanosheet was fully detached without any shape or size (approximately 4 cm^2) distortion (Fig. 1a). The resulting free-standing nanosheet floating in acetone was then washed by exchanging the acetone three times. This polysaccharide nanosheet was quite stable in acetone or

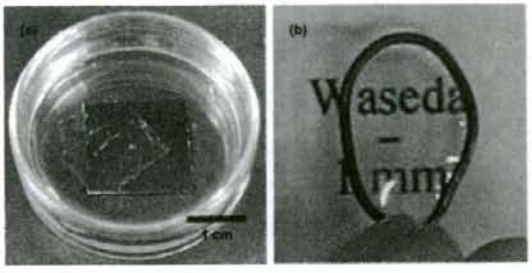

Figure 1. Microscopy image of a polysaccharide nanosheet: a) detached from the substrate and floating in acetone and b) in the air supported by a wire loop.

phosphate buffered saline (PBS, pH 7.4) solution for more than three months. Besides, it could be scooped with a wire loop just as described by Kunitake and co-workers by using a nanosheet consisting of an organic/inorganic interpenetrating network.[5d] Furthermore, no crack was observed in the nanosheet in the air (Fig. 1b). However, once the nanosheet sustained by the wire loop was damaged with a needle, it became ruptured and was immediately ruined. These results demonstrated that the nanosheet could be treated in a dried state provided that it is sustained by a frame. However, its configuration (e.g., shape and size) was restricted by the supporting frame size. Therefore, it was quite difficult to maintain the configuration of the nanosheet in the air without the supporting frame.

A floating nanosheet was put on a calcium fluoride (CaF_2) substrate for characterization of the polysaccharide nanosheet by Fourier transform infrared (FTIR) spectroscopy. By comparing the peaks attributed to the vibration mode among the chitosan hydrochloric acid, Na alginate, and the nanosheet, the main driving force building the nanosheet structure was confirmed to be electrostatic interactions and hydrogen bonding.[10] The asymmetric (band at 1627 cm^{-1}) and symmetric (band at 1523 cm^{-1}) N–H bending vibration modes of non-acylated 2-aminoglucose primary amines derived from the chitosan homopolymer were absent, indicating that the $-NH_3^+$ of the chitosan had reacted with the $-COO^-$ of the alginate by electrostatic interaction. Moreover, the band of the nanosheet at around 3000 cm^{-1}, corresponding to the O–H stretching vibration modes of the polysaccharide structure, became broader than that of the chitosan and alginate homopolymers. This observation suggested intermolecular hydrogen bonding between chitosan and alginate was enhanced over the intramolecular interaction of each homopolymer. Additionally, from the FTIR spectrum of the librated nanosheet, the novolac resin and that of the photoactive compound (diazonaphthoquinone) were barely detected in the nanosheet spectrum compared with the spectrum of the photoresist (thickness: 2.2 μm) directly spin-coated on the CaF_2 substrate. Details of the FTIR spectroscopic study of the nanosheet are given in the Supporting Information.

For the morphological study of the polysaccharide nanosheet surface, the free-standing nanosheet floating in acetone was transferred onto a fresh silicon wafer and observed by using atomic force microscopy (AFM). Large-scale (90 μm × 90 μm) topographic images shown in Figure 2a and b revealed that the nanosheet surface was as smooth and flat as the silicon wafer surface, without any corrugations and wrinkles. These topographical results were obtained because of the high-speed horizontal diffusion of the polymers during spin-coating.[4a] Furthermore, scanning the surface morphology of the polysaccharide nanosheet with a surface profiler in the range of 500 μm showed a significant difference in surface roughness (root-mean squared (RMS) values) of (1.9 ± 0.7) nm (0.5 M NaCl) and (7.1 ± 2.4) nm (0 M NaCl), although a significant difference in the thickness of the polysaccharide nanosheet was not found. Hence, the relatively high ionic strength (0.5 M NaCl) of the polyelectrolyte aqueous solution during fabrication (i.e., using the SA-LbL method) presumably weakened the electrostatic interactions of the polymers, generating a smooth flat surface as the overall morphology of the polysaccharide nanosheet.[9b]

From the cross-sectional analysis of the polysaccharide nanosheet edge, as shown in Figure 2a, the thickness of the nanosheet was estimated to be (30.2 ± 4.3) nm (Fig. 2c). This thickness is in good agreement with that determined for the nanosheet prepared on the substrate ((30.7 ± 4.5) nm), as shown by an ellipsometric analysis (see Supporting Information). Therefore, the thickness of the nanosheet was maintained before and after transference. Because the nanosheet was a LbL film directly assembled on the silicon wafer by 10.5 pairs of the polysaccharides, the thickness of one pair of the polyelectrolytes was calculated to be approximately 2.9 nm. This thickness is in good agreement with that of previously reported LbL films fabricated by the SA-LbL method using similar molecular weight (i.e., ca. 10^5) polyelectrolytes.[4] In addition, the mechanical properties of the polysaccharide nanosheet fabricated in pure water was preliminarily measured by applying air pressure as a bulge test;[5d,6a] the elastic modulus was approximately 1.3 GPa—close to the value of the free-standing polymer nanosheet (1.5 GPa) composed of poly(allylamine hydrochloride) and poly(sodium 4-styrenesulphonate), reported by Tsukruk and co-workers.[5b] (The details of the mechanical properties of the polysaccharide nanosheet are currently under investigation.) Here we

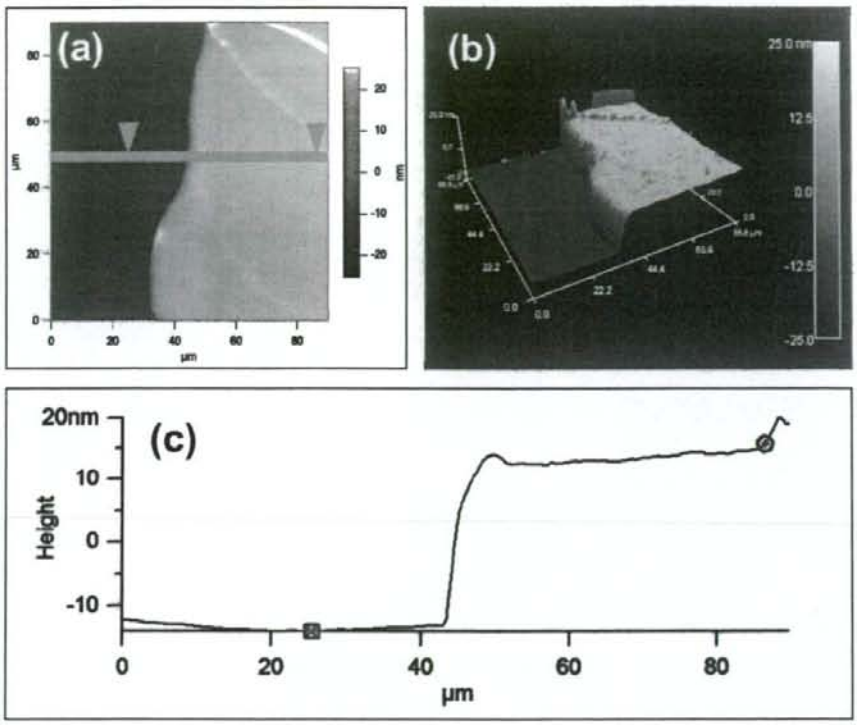

Figure 2. AFM images of the edge of the transferred polysaccharide nanosheet on a SiO_2 substrate: a) top view, b) 3D image, and c) cross-sectional image.

succeeded in the fabrication of a free-standing polysaccharide nanosheet with a high aspect ratio of size and thickness (i.e., $>10^6$).

In order to transfer this polysaccharide nanosheet from the surface of one substrate to another without distorting the overall shape, we incorporated a hydrophilic sacrificial membrane between the polysaccharide nanosheet and the substrate. We named this three-layered composite film a nano-adhesive plaster because we envisaged the nanosheet could attach to skin and the substrate was subsequently peeled off by the dissolution of the sacrificial membrane using water.

The nano-adhesive plaster was prepared by using the method described in the Experimental section (see Fig. 3a). In order to transfer the polysaccharide nanosheet from the substrate onto human skin, we prepared a polyvinyl alcohol (PVA) membrane as a hydrophilic sacrificial membrane. We chose PVA as a suitable material for the sacrificial membrane because it is a water-soluble polymer that does not adversely affect the skin. Owing to its flexibility, silicon rubber was chosen as a substrate for the PVA membrane. The PVA membrane was prepared by spin-coating a 20 wt % PVA aqueous solution on a polypropylene (PP) substrate. The PVA membrane, approximately 1.2 μm thick (measured by surface profiler), was then spontaneously released from the acetone-insoluble PP substrate within a few seconds by immersion in acetone. The free-standing PVA membrane was robust and compliant in acetone when picked up with tweezers. We also tested several flexible polymeric substrates that are insoluble or poorly soluble in acetone, such as polyethylene terephthalate, silicon rubber, and polyvinylchloride. However, PVA was repelled by all of them because of the intermediate hydrophilic–hydrophobic surface of the PP substrate. The free-standing PVA membrane floating in acetone was scooped out and then transferred onto the silicone rubber substrate.

With the resulting PVA–silicone rubber substrate, the polysaccharide nanosheet, modified with a small amount of commercialized luminescent pigment for ease of visibility in the dark, was scooped onto the air–solid surface. As a result, three kinds of free-standing sheets with different thickness were assembled to fabricate the nano-adhesive plaster; silicone rubber on a milliscale (1.0 mm), PVA membrane on a microscale (1.2 μm), and a polysaccharide nanosheet on a nanoscale (30 nm) (Fig. 3b). A luminescent-labeled nanosheet was clearly observed in the dark as a square shape, and no cracks or deformations were observed in the nanosheet over a period of a few months when stored at the ambient

ADVANCED MATERIALS

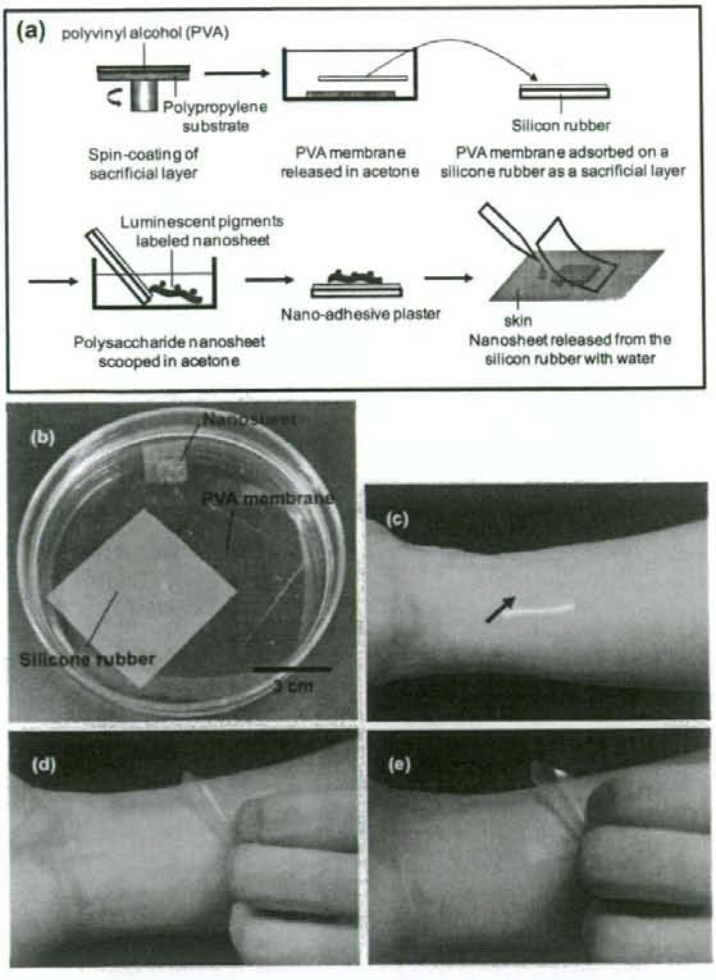

Figure 3. a) Schematic illustration showing the fabrication of a nano-adhesive plaster. b) Three kinds of free-standing sheets floating in acetone, photographed in the dark; the surface of polysaccharide nanosheet was modified with luminescent pigment for ease of visibility. A nano-adhesive plaster on the human skin c) before the polysaccharide nanosheet was released from the silicone rubber and d) after release from the silicone rubber. (e) is the same image as (d) except that it was captured in the dark.

temperature. Although the surface roughness of the PVA membrane was much higher (RMS: (129±98) nm) than that of the polysaccharide nanosheet, any deformation caused by the surface roughness was not found in the polysaccharide nanosheet, suggesting that the polysaccharide nanosheet was stable and fitted on the surface of the PVA membrane with good flexibility. Moreover, the surface roughness of the PVA membrane did not affect that of the polysaccharide nanosheet when the polysaccharide nanosheet was released from the silicone rubber because the PVA membrane was dissolved easily by water.

To test the practical applications of the nano-adhesive plaster, we attached it to the skin on the right arm of a human subject. Prior to transference of the polysaccharide nanosheet from the PVA-silicone rubber substrate onto the skin, the contour on the nanosheet surface was observable because of differences in reflectivity (Fig. 3c arrow). The polysaccharide nanosheet was then released from the PVA-silicone rubber substrate within a few seconds by the dissolution of the PVA layer with a drop of 500 μL deionized (DI) water through a micropipette. The nanosheet on the skin was barely visible from the top view under visible light (Fig. 3d). Luminescent signals from the modified nanosheet confirmed that the shape and size of the polysaccharide nanosheet were preserved on the skin. Furthermore, luminescent regions were barely detected on the removed silicone rubber side, demonstrating the successful transference of the nanosheet onto the skin (Fig. 3e). Moreover, the configuration of the polysaccharide nanosheet was stable for at least 24 h, despite perspiration from the skin and the possibility of it being rinsed away by washing with soap. These results indicated that the polysaccharide nanosheet was released from the silicone rubber by dissolution of the PVA layer with a drop of water and completely transferred onto the skin. The polysaccharide nanosheet was no longer visible on the skin, perhaps because the surface relief of the skin perfectly matched that of the flexible sheet at the nanometer scale. Considering the high biocompatibility and biodegradability of the LbL ultrathin films composed of chitosan and Na alginate reported by some research groups,[11] it is likely that the free-standing polysaccharide nanosheet will be applied in biological systems.

In conclusion, we successfully constructed polymer nanosheets (30 nm thick) comprising the biocompatible and biodegradable polysaccharide-electrolytes with a high aspect ratio of size to thickness (>10^6). Furthermore, we demonstrated transference of the polysaccharide nanosheet from the silicone rubber substrate onto a human skin surface by fabricating a three-layered nano-adhesive plaster. By ubiquitous

transference of the free-standing polymer nanosheet, ultrathin films have been freed from the conventional solid substrate and the advantages of having the films alone at various interfaces, such as human skin, as shown in this report can now be explored. We estimate that the polysaccharide nanosheet would show similar biocompatibility and biodegradability. To our knowledge, this is the first report to show the potential application of free-standing polymer nanosheets in the field of biomedical research. Particularly, the invisible nanosheet on the skin will have obvious applications in the field of skincare. We are currently investigating further the physical and biomedical properties of the polysaccharide nanosheet, such as mechanical strength, biocompatibility, and biodegradability at a cellular level. These results will be reported shortly.

Experimental

The biodegradable polyelectrolytes, chitosan (M_w = 88 kDa; 1 Da = 1.66×10^{-27} kg) and sodium alginate (Na Alginate, M_w = 106 kDa) were purchased from Nacalai Tesque., Inc. (Kyoto, Japan). OFPR-800 LB photoresist (200 cP) and PVA (M_w = 22 kDa) were purchased from Tokyo Ohka Kogyo Co. Ltd. (Kanagawa, Japan) and Kanto Chemical Co., Inc. (Tokyo, Japan), respectively. Silicon wafers purchased from KST World Co. (Fukui, Japan), cut to a size of 20 mm × 20 mm, were immersed in a mixture of sulfuric acid/hydrogen peroxide (3:1) for 10 min and then thoroughly rinsed with DI water (18 MΩ cm). A CaF_2 substrate for FTIR analysis was purchased from Sigma Koki Co., ltd. (Tokyo, Japan). Luminescent pigment was purchased from Sinloihi Co., ltd. (Kanagawa, Japan). Chitosan (1 mg mL^{-1}, 1 % acetic acid, 0.5 M NaCl) and Na alginate (1 mg mL^{-1}, 0.5 M NaCl) solutions were prepared with DI water. All routines for nanosheet fabrication were conducted in a clean room (class 10 000 conditions) to avoid contamination.

The free-standing polysaccharide nanosheet was fabricated by using a SA-LbL method as described in the literature [4c]. A 150 μL solution of the polyelectrolyte was dropped onto the substrates and then the substrate was rotated at 4500 rpm for 15 s. Then the substrate was rinsed twice with DI water and dried by spinning (ca. 30 s). The nanosheets were prepared in the following steps (under the above conditions): a) spin-coating the photoresist layer (800 rpm, 3 s and 7000 rpm, 20 s); b) deposition of the chitosan layer (20 min) by physical adsorption; c) repetition of the chitosan and Na alginate multilayering by using the SA-LbL method (4500 rpm, 15 s for each polyelectrolyte); d) termination of the SA-LbL at the chitosan spin-coating stage; e) immersion of the resulting polysaccharide nanosheet adsorbed on the substrate for dissolution of the underlying resist layer in acetone.

For fabrication of a nano-adhesive plaster, a free-standing PVA membrane as a sacrificial layer was prepared by spin-coating (800 rpm, 3 s and 7000 rpm, 20 s) a PVA aqueous solution (20 wt %) onto a PP substrate (5 cm × 5 cm). The PVA layer was released in acetone and transferred onto a piece of flexible silicone rubber. The polysaccharide nanosheet adsorbed on the substrate, before immersion in acetone, was immersed into an aqueous dispersion of commercialized luminescent pigment for 20 min. A small amount of luminescent pigment was present on the surface of the nanosheet. Then the luminescent pigment-labeled nanosheet was released in acetone from the substrate and transferred onto the surface of the PVA-silicone rubber. Sequentially, the nanosheet was transferred onto the human skin by dissolution of the PVA membrane with 500 μL of water.

The polysaccharide nanosheets were photographed using a digital camera OLYMPUS C-5050 ZOOM (Olympus Co., Tokyo, Japan). Surface morphology was observed by using AFM in the tapping mode (MFP-3D-BIO, Asylum Research Co., Santa Barbara, CA). A stokes ellipsometer (Gaertner Scientific Co., Skokie, IL) was also used to measure the thickness of the nanosheet. The wide-range surface roughness of the PVA membrane as well as that of the polysaccharide nanosheets was measured with a surface profiler α-step (KLA-Tencor Corp., San Jose, CA). Characterization of the free-standing nanosheet was confirmed by using a FTIR-410 device (JASCO Corp., Tokyo, Japan).

Received: March 20, 2007
Revised: July 27, 2007

[1] a) Y. Lvov, G. Decher, H. Mohwald, *Langmuir* **1993**, *9*, 481. b) Y. Lvov, K. Ariga, I. Ichonose, T. Kunitake, *J. Am. Chem. Soc.* **1995**, *117*, 6117. c) G. Decher, Y. Lvov, J. Schmitt, *Thin Solid Films* **1994**, *244*, 772. d) V. V. Tsukruk, V. N. Bliznyuk, D Visser, A. L. Campbell, T. J. Buning, W. W. Adams, *Macromolecules* **1997**, *30*, 6615. e) G. Decher, *Science* **1997**, *277*, 1232. f) *Multilayer Thin Films* (Eds: G. Decher, J. B. Schlenoff), Wiley-VCH, Weinheim, Germany **2003**.

[2] a) T. Serizawa, M. Tamaguchi, M. Akashi, *Biomacromolecules* **2002**, *3*, 724. b) L. Zhai, F. C. Cobeci, R. E. Cohen, M. F. Rubner, *Nano Lett.* **2004**, *4*, 1349. c) K. Sano, H. Sasaki, K. Shibata, *J. Am. Chem. Soc.* **2006**, *128*, 1717. d) C. Jiang, V. V. Tsukruk, *Adv. Mater.* **2006**, *18*, 829. e) Z. Tang, Y. Wang, P. Podsiadlo, N. A. Kotov, *Adv. Mater.* **2006**, *18*, 3203.

[3] a) F. Caruso, R. A. Caruso, H. Mohwald, *Science* **1998**, *282*, 1111. b) C. Gao, S. Moya, E. Donath, H. Mohwald, *Macromol. Chem. Phys.* **2002**, *203*, 953.

[4] a) J. Cho, K. Char, J. Hong, K. Lee, *Adv. Mater.* **2001**, *13*, 1076. b) J. Cho, K. Char, *Langmuir* **2004**, *20*, 4011. c) C. Jiang, S. Markutsya, V. V. Tsukruk, *Adv. Mater.* **2004**, *16*, 157.

[5] a) A. A. Mamedov, N. A. Kotov, *Langmuir* **2000**, *16*, 5530. b) C. Jiang, S. Markutsya, Y. Pikus, V. V. Tsukruk, *Nat. Mater.* **2004**, *3*, 721. c) Y. Kado, M. Mitsuishi, T. Miyashita, *Adv. Mater.* **2005**, *17*, 1857. d) R. Vendamme, S. Onoue, A. Nakao, T. Kunitake, *Nat. Mater.* **2006**, *5*, 494. e) H. Endo, Y. Kado, M. Mitsuishi, T. Miyashita, *Macromolecules* **2006**, *39*, 5559. f) S. S. Ono, G. Decher, *Nano Lett.* **2006**, *6*, 592.

[6] a) S. Markutuya, C. Jiang, Y. Pikus, V. V. Tsukruk, *Adv. Funct. Mater.* **2005**, *15*, 771. b) C. Jiang, S. Singamaneni, E. Merrick, V. V. Tsukruk, *Nano Lett.* **2006**, *6*, 2254. c) C. Jiang, M. E. McConney, S. Singamaneni, E. Merrick, Y. Chen, J. Zhao, L. Zhang, V. V. Tsukruk, *Chem. Mater.* **2006**, *18*, 2632.

[7] a) M. N. V. R. Kumar, R. A. A. Muzzarelli, C. Muzzarelli, H. Sashiwa, A. J. Domb, *Chem. Rev.* **2004**, *104*, 6017. b) H. Yi, L. Wu, W. E. Bentley, R. Ghodssi, G. W. Rubloff, J. N. Culver, G. F. Payne, *Biomacromolecules* **2005**, *6*, 2881. c) I. Liao, A. C. A. Wan, E. K. >F. Yim, K. W. Leong, *J. Controlled Release.* **2005**, *104*, 347.

[8] a) T. Serizawa, M. Yamaguchi, M. Akashi, *Biomacromolecules* **2002**, *3*, 724. b) Z. Tang, Y. Wang, P. Podsiadlo, N. A. Kotov, *Adv. Mater.* **2006**, *18*, 3203.

[9] a) S. L. Clark, M. F. Motague, P. T. Hammond, *Macromolecules* **1997**, *30*, 7237. b) J. Cho, H. Jang, B. Yeom, H. Kim, R. Kim, S. Kim, K. Char, F. Caruso, *Langmuir* **2006**, *22*, 1356.

[10] M. G. Sankalia, R. C. Mashru, J. M. Sankalia, V. B. Sutariya, *Eur. J. Pharm. Biopharm.* **2007**, *65*, 215-232.

[11] a) Y. Yang, Q. He, L. Duan, Y. Cui, J. Li, *Biomaterials* **2007**, *28*, 3083. b) A. L. Hillberg, M. Tabrizian, *Biomacromolecules* **2006**, *7*, 2742.

J Artif Organs (2006) 9:251–258
DOI 10.1007/s10047-006-0345-0

ORIGINAL ARTICLE

Yosuke Okamura, PhD · Makoto Handa, MD, PhD
Hidenori Suzuki, PhD · Yasuo Ikeda, MD, PhD
Shinji Takeoka, PhD

New strategy of platelet substitutes for enhancing platelet aggregation at high shear rates: cooperative effects of a mixed system of fibrinogen γ-chain dodecapeptide- or glycoprotein Ibα-conjugated latex beads under flow conditions

Abstract To construct platelet substitutes that have hemostatic properties over a wide range of shear rates, we used fibrinogen γ-chain carboxy-terminal sequence HHLGGAKQAGDV (H12), which recognizes activated platelets at low shear rates, and a recombinant water-soluble moiety of the platelet glycoprotein (rGPIbα), which recognizes von Willebrand factor at high shear rates. Three kinds of samples were prepared for this purpose: H12-conjugated latex beads (H12-latex beads), rGPIbα-latex beads, and H12/rGPIbα-latex beads. These samples were evaluated in thrombocytopenia-imitation blood at various flow conditions. Based on ADP-induced platelet aggregation studies, the H12-latex beads significantly enhanced platelet aggregation via H12 binding with GPIIb/IIIa activated on the surface of activated platelets, whereas the rGPIbα-latex beads did not support platelet aggregation. In the case of the H12/rGPIbα-latex beads, the function of H12 was suppressed by steric hindrance from the larger rGPIbα bound to the latex bead. A mixture of the H12-latex beads and the rGPIbα-latex beads adhered to a collagen surface over a wide range of shear rates. In particular, at high shear rates, a cooperative effect was observed in the enhancement of platelet thrombus formation compared with H12-latex beads or rGPIbα-latex beads alone. We propose that a mixed system of H12- and rGPIbα-conjugated nanoparticles is a more effective platelet substitute than each of the beads used alone and has enhanced platelet aggregation properties.

Key words Platelet substitute · Fibrinogen γ-chain dodecapeptide · Platelet glycoprotein (GP) Ibα · Thrombocytopenia-imitation blood · Shear rate

Received: October 27, 2005 / Accepted: June 12, 2006

Y. Okamura · S. Takeoka (✉)
Graduate School of Science and Engineering, Waseda University, Tokyo 169-8555, Japan
Tel. +81-3-5286-3217; Fax +81-3-5286-3217
e-mail: takeoka@waseda.jp

Y. Okamura · M. Handa
Department of Transfusion Medicine and Cell Therapy, School of Medicine, Keio University, Tokyo, Japan

H. Suzuki
Center for Electron Microscopy, Tokyo Metropolitan Institute of Medical Science, Tokyo, Japan

Y. Ikeda
Department of Internal Medicine, School of Medicine, Keio University, Tokyo, Japan

Introduction

Platelet transfusion plays an important role in the supportive therapy of thrombocytopenia caused by cancer or hematologic malignancies, or in the perioperative period. However, a shortage of platelet concentrates has always been a serious issue because of the short storage period (3 days in Japan), insufficient donations, and the imbalance of demand and supply. Furthermore, there is the issue of the risk of viral and bacterial infections from transfusion. For these reasons, a number of trials have been conducted to develop platelet substitutes such as infusible platelet membranes (IPMs),[1] solubilized platelet membrane protein-conjugated liposomes (plateletsomes),[2] fibrinogen-bonded red blood cells,[3] fibrinogen-coated albumin microcapsules (synthocytes),[4] and arginine-glycine-asparaginic acid (RGD) peptide-bound red blood cells (thromboerythrocytes).[5] However, these platelet substitutes consist of materials derived from blood components.

We also conjugated fibrinogen[6] to biocompatible carriers such as polymerized albumin particles (polyAlb)[7–9] and phospholipid vesicles (liposomes).[10–13] Fibrinogen conjugates facilitated platelet aggregation on an activated platelet-immobilized surface in vitro by the recruitment of flowing platelets in the aggregates after their attachment.[6] However, fibrinogen isolated from human blood tends to precipitate at 4°C within a few hours.[6] Recently, we have focused on fibrinogen dodecapeptide (HHLGGAKQAGDV; H12)[14–18] and confirmed that the H12-conjugates showed minimal interaction with

nonactivated platelets[19] and enhanced in vitro platelet thrombus formation on a collagen-immobilized plate under the flow of thrombocytopenia-imitation blood.[9,19] However, this effect was limited to low shear rates (e.g., $150\,s^{-1}$).

We also developed the water-soluble part of GPIbα as a recombinant product (rGPIbα) as a key recognition site of platelet substitutes.[20–22] In previous studies we found that rGPIbα-polyAlb accumulated on the von Willebrand factor (VWF)-immobilized surface at high shear rates (e.g., $1600\,s^{-1}$),[10] reflecting the interaction of natural GPIbα with VWF.[23–26] Therefore, we consider that H12- or rGPIbα-particles alone would not be effective for the recognition of the sites of vascular injury over a wide range of shear rates.

In this study, we selected H12 and rGPIbα as recognition sites for platelet substitutes and prepared four kinds of samples: H12/rGPIbα-latex beads, with conjugated H12 and rGPIbα both on the same latex bead, H12-latex beads, rGPIbα-latex beads, and a mixture of H12-latex beads and rGPIbα-latex beads. Latex beads are very useful carriers for in vitro studies because of their uniform size and ease of visualization by microscopic observation.

Materials and methods

Reagents

Fibrinogen γ-chain dodecapeptide with an added cysteine to the amino-terminal (H12: C-HHLGGAKQAGDV) was synthesized using a solid-phase synthesizer from BEX (Tokyo, Japan). Latex beads (Polybead or Fluoresbrite, 1 μm in diameter) and *N*-succinimidyl 3-(2-pyridyldithio) propionate (SPDP) were purchased from Polysciences (Warrington, PA, USA) and Pierce (Rockford, IL, USA), respectively. An anticoagulant D-Phe-Pro-Arg-chloromethylketone (PPACK) was purchased from Calbiochem (San Diego, CA, USA). 3,3′-Dihexyloxacarbocyanine iodide ($DiOC_6$), which is a platelet fluorescent dye, was purchased from Molecular Probes (Eugene, OR, USA). The monoclonal antibodies against rGPIbα, GUR20-5, and horseradish peroxidase-conjugated GUR83-35 were purchased from Takara Bio (Otsu, Japan). Recombinant human serum albumin (rHSA) and purified rGPIbα were kindly donated by Mitsubishi Pharma (Osaka, Japan).

Preparation of H12- or rGPIbα-conjugated latex beads

Latex beads bearing H12. Latex beads were mixed with an rHSA solution (50 mg/ml) and incubated at room temperature for 2 h to coat the surface of the latex beads with rHSA. After the separation of the remaining rHSA by centrifugation (13000*g*, 5 min, 4°C, three times), the rHSA-coated latex beads were suspended in phosphate-buffered saline (PBS, pH 7.4). A solution of SPDP in ethanol (5 mM, 5 μl) was added to the suspension of the latex beads (4.0×10^6/μl) and incubated for 30 min at room temperature. The unreacted SPDP and the by-products were separated by centrifugation and the pyridyl disulfide (PD)-bonded rHSA-coated latex beads were collected. A suspension of the latex beads (4.0×10^6/μl) was mixed with a solution of H12 (10 mM, 8 μl) and reacted at 25°C for 12 h, undergoing the thiol-disulfide exchange reaction. The unreacted H12 was removed by centrifugation to purify the latex beads bearing H12 (H12-latex beads, 2.0×10^6/μl). The concentration of the H12 conjugated to the latex beads was determined by indirect quantification of the 2-thiopyridone (2TP) that was liberated during the thiol-disulfide exchange reaction using high-pressure liquid chromatography (HPLC) on a TSK-GEL G3000SW_{XL} (Tosoh, Tokyo, Japan) column (7.8 mm outside diameter (o.d.) × 300 mm height in PBS at 1 ml/min), by measuring the absorbance of the column flow at 343 nm.

Latex beads bearing rGPIbα. A solution of SPDP in ethanol (5 mM, 5 μl) was added to an rGPIbα solution (4.3 mg/ml, 200 μl) and incubated for 20 min at room temperature. A dithiothreitol solution (final concentration: 20 mM) was added to the PD-rGPIbα solution to obtain SH-rGPIbα after separation with gel permeation chromatography (GPC) (sephadex G25). The solution of the SH-rGPIbα (1.0 mg/ml) was mixed with a suspension of the PD-bonded rHSA-coated latex beads, obtained as described above, and reacted at 25°C for 12 h. The unreacted reagents were removed by centrifugation to separate the latex beads bearing rGPIbα (rGPIbα-latex beads, 2.0×10^6/μl). The concentration of the rGPIbα conjugated on the latex beads was determined with a sandwich enzyme-linked immunosorbent assay (ELISA) with GUR20-5 and horseradish peroxidase-conjugated GUR83-35.[19]

Latex beads bearing both H12 and rGPIbα. A solution of SPDP in ethanol (20 mM, 10 μl) was added to a suspension of rHSA-coated latex beads (4.0×10^6/μl) and incubated for 30 min at room temperature. A suspension of the PD-latex beads (4.0×10^6/μl) was mixed with an aqueous solution of H12 (4 mM, 8 μl) and reacted at 25°C for 12 h. The unreacted reagents were removed by centrifugation and the purified H12-latex beads (2.0×10^6/μl) were obtained. SH-rGPIbα solution (1 or 2 ml, 1.0 mg/ml) was added to the dispersion of the H12-latex beads and incubated for 12 h at room temperature. The latex beads bearing both H12 and rGPIbα (H12/rGPIbα-latex beads) were purified by centrifugation. The concentration of H12 or rGPIbα conjugated on the latex bead was determined by HPLC or a sandwich ELISA, respectively, as described above.

Platelet aggregation study

Blood withdrawn from healthy volunteers was mixed with 10% volume of 3.8% (w/v) sodium citrate. Platelet-rich plasma (PRP) was prepared by centrifugation (100*g*, 15 min, 22°C), and the platelet concentration of PRP was adjusted to 2.0×10^5/μl with platelet-poor plasma (PPP) prepared by centrifugation (2200*g*, 10 min, 22°C). The platelet concentration was determined using an automated

hematology analyzer (K-4500, Sysmex, Kobe, Japan). An ADP solution was added to the PRP containing H12-latex beads or H12/rGPIbα-latex beads (final concentrations, $2.0 \times 10^3/\mu l$) at a final concentration of ADP of 3μM, and the light transmittance was measured with an aggregometer (Hema Tracer T-638, Nico Bioscience, Tokyo, Japan).

Preparation of the collagen-immobilized surface

Collagen I-A (3.0 mg/ml, Cellmatrix, Nitta Gelatin, Osaka, Japan) was suspended in PBS at 4°C to give a final concentration of 30μg/ml. Glass plates (diameter 24 mm, thickness 0.5 mm) were immersed in the collagen suspension at 4°C for 8h, were carefully rinsed with PBS, and then immersed in a bovine serum albumin solution (20 mg/ml) at 20°C for 2h.

Measurement of the interaction of platelets and the H12- or rGPIbα-latex beads with the collagen surface

Blood, which was treated with thrombin inhibitor PPACK (final concentration, 40μM), was filtered with a leukocyte removal filter (NEO1J, Nihon Poll, Tokyo, Japan) to remove platelets as well as leukocytes. The residual platelet concentration of the filtered blood was determined to be $(6.0 \pm 2.0) \times 10^3/\mu l$, and the final platelet concentration was adjusted to $2.0 \times 10^4/\mu l$ by the addition of PRP. The platelet concentration was determined using an automated hematology analyzer (K-4500). Blood thus prepared was termed thrombocytopenia-imitation blood.

In the perfusion study, either platelets or the latex beads were labeled with a fluorescent marker [platelets: $DiOC_6$, latex beads: Fluorescein-4-isothiocyanate (FITC)]. The thrombocytopenia-imitation blood in the presence of the H12- or rGPIbα-latex beads ($1.0 \times 10^8/\mu l$) was placed in a recirculating chamber mounted on an epifluorescence microscope (ECLIPS TE300, Nikon, Tokyo, Japan) equipped with a CCD camera, and the interaction of the platelets or latex beads with the collagen immobilized on the surface was observed at 37°C. The surface coverage of platelets or H12- or rGPIbα-latex beads on the plates was calculated with an Argus-20 image processor (Hamamatsu Photonics, Hamamatsu, Japan). All measurements were performed in triplicate, and the results are shown as an average surface coverage with the three experimental values given in brackets.

Observation of the H12-latex beads or the rGPIbα-latex beads adhering on the platelet thrombus using a scanning electron microscope

Aggregates of platelets and latex beads adhering on the glass plates after the perfusion study were washed with a Hepes buffer (pH 7.4), fixed with 1% (v/v) glutaraldehyde (Electron Microscopy Sciences, Fort Washington, PA, USA) in 0.1M phosphate buffer (pH 7.4) for 30 min, and postfixed with 1% (w/v) osmium tetroxide in the same buffer for 30 min. The samples were dehydrated with a graded ethanol series and then dried in a freeze-dryer (Hitachi ES-2020, Hitachi, Tokyo, Japan) using *t*-butyl alcohol. For immunostaining, the plates were incubated with 0.1% (w/v) bovine serum albumin in PBS for blocking. They were incubated with mouse antihuman GPIb/IX antibody (SZ2, Immunotech, 10μg/ml, PBS) at 4°C overnight. The plates were washed three times with PBS and incubated with goat-antihuman IgG coupled to colloidal gold (Amersham Bioscience, 15 nm, 1:100 final dilution) at room temperature for 60 min. After coating with osmium tetroxide (ca. 5 nm thick) using an osmium plasma coater (NL-OPC80, Nippon Laser and Electronics, Nagoya, Japan), the samples were examined with a Hitachi S-4500 field emission scanning electron microscope (SEM) at an accelerating voltage of 7 kV.[27] Colloidal gold-labeled latex beads on the platelet thrombus (number of thrombi: 120) were counted as the rGPIbα-latex beads, and the nonlabeled latex beads were counted as H12-latex beads. The glass plates were marked to distinguish the direction of blood flow, which was from left to right of the SEM image.

The location of each bead on the platelet thrombus, as shown in Fig. 4a, was determined as follows. First, we drew a line connecting the center of a thrombus and the center of a latex bead. Second, from the point where the line met the thrombus edge, a tangent line was drawn. Finally, a second line (1) was drawn parallel to the tangent line that passed through the center of the latex bead.

Next, we determined the blood flow as a vector and we drew a reflected vector from the point where the incident vector intersected with line (1). The reflected vector was resolved into X and Y components. We defined the position of a latex bead as "front" when the X component was negative and "side" when the X component was positive. Furthermore, any latex bead located on the downstream side of the thrombus (the blood flow vector did not directly collide with the latex beads), we defined as located on the "back".

Results

Characterization of the H12-latex beads, the rGPIbα-latex beads, and the H12/rGPIbα-latex beads

The mercapto group attached to the N-terminal of H12 as cysteine was reacted with the PD group conjugated to the lysine residues of rHSA, which was physically absorbed on the surface of the latex bead. The number of H12 molecules conjugated to one latex bead was estimated to be approximately 2.0×10^5 by HPLC. Similarly, the mercapto group of rGPIbα was conjugated to the latex beads via a disulfide linkage with the rHSA absorbed on the latex bead. The number of rGPIbα molecules on the surface of a latex bead was calculated to be approximately 1.0×10^4. In the preparation of the H12/rGPIbα-latex beads, SH-rGPIbα molecules were reacted with the PD group (approximately 1.0×10^5/particle) remaining on the surface of the H12-latex beads. However, the resulting number of rGPIbα molecules

did not reach 1.0×10^4 and was estimated to be 5.0×10^3, despite the addition of excess SH-rGPIbα compared with the rGPIbα. In this study, two preparations of the H12/rGPIbα-latex beads were used. One preparation was estimated to contain 1.7×10^3 molecules of rGPIbα per bead and the other 5.0×10^3 molecules per bead.

Platelet aggregation study

Using an aggregometer, we confirmed the function of H12 on the H12-latex beads and the H12/rGPIbα-latex beads as shown in Fig. 1. In the case of the control albumin-absorbed latex beads, the transmittance of ADP-induced platelet aggregation was 40% (Fig. 1a). When the H12-latex beads were added instead of the control, the transmittance increased significantly to approximately 70% (Fig. 1b). In the case of the H12/rGPIbα-latex beads, the increase in transmittance was considerably smaller and the transmittance approached the control value, especially for the H12/rGPIbα-latex beads conjugated with the large number of rGPIbα molecules (Fig. 1c,d). The rGPIbα-latex beads showed the same transmittance as the control (data not shown).

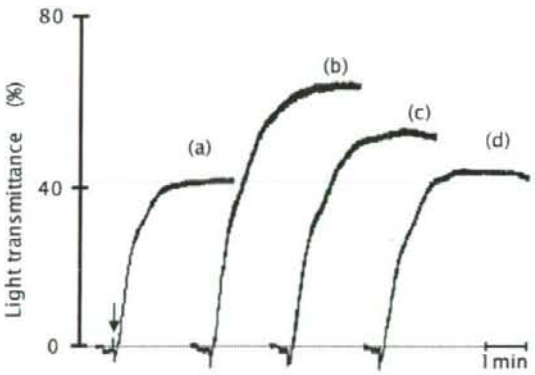

Fig. 1. ADP-induced (3 μM) platelet (final count: 2.0×10^5/μl) aggregation in the presence of latex bead samples: *a* noncoated latex beads, *b* HHLGGAKQAGDV-(H12)-latex beads, *c* and *d* H12/rGPIbα-latex beads). The final concentration of beads was 2.0×10^5/μl. The number of H12 molecules conjugated to one latex bead was *a* 0, and *b*–*d* 2.0×10^3. The number of rGPIbα molecules conjugated to one latex bead was *a* 0, *b* 0, *c* 1.7×10^3, and *d* 5.0×10^3. *Arrow* shows addition of ADP

The interaction of platelets and H12- and rGPIbα-latex beads with a collagen surface

We studied a mixture of H12-latex beads and rGPIbα-latex beads, both of which were labeled with FITC and were allowed to flow over a collagen surface at various shear rates. We used thrombocytopenia-imitation blood in which the total number of platelets and latex beads was adjusted to 2.0×10^4/μl and 1.0×10^5/μl, respectively. At first, we confirmed that no adhesion was observed at various shear rates when the control latex beads were allowed to flow, as shown in Fig. 2a (●). When the H12-latex beads were made to flow over the surface instead of the control beads at a shear rate of $150 s^{-1}$, the average surface coverage after 3 min tended to increase to 5.1% [3.9%, 4.9%, 6.6%]. The average surface coverage decreased with increasing shear rate to 1.2% [0.7%, 1.2%, 1.6%] at $800 s^{-1}$ and 1.0% [0.3%, 1.1%, 1.7%] at $1600 s^{-1}$ [Fig. 2a (◊)]. In contrast, the rGPIbα-latex beads adhered immediately and accumulated on the collagen surface. The average surface coverage of the rGPIbα-latex beads increased with increasing shear rate and was 2.8% [2.1%, 3.0%, 3.4%] at $150 s^{-1}$, 4.3% [3.2%, 3.9%, 5.8%] at $800 s^{-1}$, and 5.0% [4.1%, 5.0%, 5.8%] at $1600 s^{-1}$ [Fig. 2a (△)]. For a mixture of H12- and rGPIbα-latex beads, the arithmetic mean surface coverage was calculated to be 4.0% [3.5%, 3.7%, 4.8%] at $150 s^{-1}$, 2.8% [2.0%, 2.8%, 3.5%] at $800 s^{-1}$, and 3.0% [2.9%, 3.0%, 3.1%]

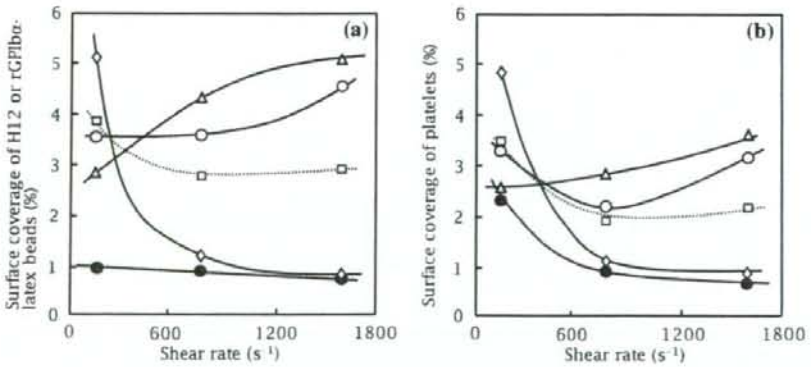

Fig. 2. Average surface coverage of **a** latex beads samples or **b** thrombocytopenia-imitation blood (platelet count: 2.0×10^4/μl) mixed with sample latex beads and passed over the surface: control latex beads (●, 1.0×10^5/μl), H12-latex beads (◊, 1.0×10^5/μl), rGPIbα-latex beads (△, 1.0×10^5/μl), a mixture of H12-latex beads (5.0×10^4/μl) and rGPIbα-latex beads (5.0×10^4/μl) (○), and calculated value of $((◊ + △)/2)$ at various shear rates (□). The average surface coverage was calculated after blood was circulated for 180 s. All measurements were performed in triplicate

at 1600s^{-1} [Fig. 2a (□)]. However, when a mixture of H12-latex beads (5.0×10^4/μl) and the rGPIbα-latex beads (5.0×10^4/μl) was used, the surface coverage was greater than the theoretical arithmetic mean surface coverage with increasing shear rate, although the change in coverage was not significant. The average surface coverage was 3.5% [2.2%, 3.7%, 4.5%] at 150s^{-1}, 3.7% [2.9%, 3.4%, 4.9%] at 800s^{-1}, and 4.6% [3.9%, 4.1%, 5.9%] at 1600s^{-1} [Fig. 2a (○)].

Next, we evaluated the adhesion and aggregation of platelets labeled with $DiOC_6$ instead of labeled latex beads under the same experimental conditions as above. In the presence of the control latex beads, the average surface coverage of platelets was 2.3% [1.2%, 2.2%, 3.6%] at a shear rate of 150s^{-1}, and this gradually decreased with increasing shear rate to 1.0% [0.3%, 1.1%, 1.7%] at 800s^{-1} and 0.8% [0.5%, 0.6%, 1.4%] at 1600s^{-1} [Fig. 2b (●)]. In the absence of the control beads, the coverage did not change at all under all observed shear rates (data not shown). When the H12-latex beads were made to flow over the collagen surface, the platelet surface coverage tended to increase to 4.8% [3.3%, 5.2%, 6.0%] at a low shear rate of 150s^{-1} and gradually decreased with increasing shear rate to 1.1% [0.7%, 1.2%, 1.5%] at 800s^{-1} and 1.0% [0.4%, 0.5%, 2.2%] at 1600s^{-1} [Fig. 2b (◊)]. In contrast, in the presence of the rGPIbα-latex beads, the platelet surface coverage increased with increasing shear rate: 2.4% [1.8%, 1.9%, 3.4%] at 150s^{-1}, 2.8% [1.3%, 3.2%, 3.8%] at 800s^{-1}, and 3.7% [2.7%, 3.8%, 4.5%] at 1600s^{-1} [Fig. 2b (△)]. The arithmetic mean platelet surface coverage for a mixture of H12-latex beads and rGPIbα-latex beads was 3.6% [2.6%, 3.5%, 4.7%] at 150s^{-1}, 1.9% [1.2%, 1.9%, 2.6%] at 800s^{-1}, and 2.3% [1.5%, 2.1%, 3.4%] at 1600s^{-1} [Fig. 2b (□)]. Although the platelet surface coverage of the mixed system did not change from the arithmetic mean surface coverage, especially at a low shear rate such as 150s^{-1} (3.3% [2.6%, 2.8%, 4.6%]), the surface coverage tended to be higher than that of the arithmetic mean as the shear rate increased: 2.2% [1.6%, 2.2%, 2.9%] at 800s^{-1} and 3.2% [2.0%, 2.2%, 4.7%] at1600s^{-1} [Fig. 2b (○)].

H12-latex beads were labeled with fluorescent marker FITC to monitor the time-course of adhesion of the H12-latex beads in the mixed system at a shear rate of 1600s^{-1}. The control latex beads did not adhere to the collagen on the plate, as shown in Fig. 3 (□). The H12-latex beads did not initially adhere to the plate; however, the average surface coverage slightly increased to 1.8% [1.5%, 1.8%, 2.2%] after 4 min of flow [Fig. 3 (△)]. In the case of the mixed system of rGPIbα-latex beads and H12-latex beads, the initial binding rate of the H12-latex beads was small and then tended to increase with time, reaching 4.2% [3.2%, 4.1%, 5.2%] after 4 min [Fig. 3 (○)].

Evaluation of adherence of H12-latex beads or rGPIbα-latex beads on the platelet thrombus by immunogold scanning electron microscopy

By immunogold scanning electron microscopy, we could immunocytochemically distinguish the rGPIbα-latex beads from the H12-latex beads adhering on the platelet thrombus in the mixed system after exposure to flow at a shear of 1600s^{-1}. The average number of each type of latex bead adhering to one thrombus was determined. There were abundant platelet thrombi with adhering latex beads, and the total number of the latex beads adhering on one thrombus was estimated to be 6.5 ± 2.6 particles (Fig. 4b). The rGPIbα-latex beads adhered approximately three times more frequently than the H12-latex beads. Next, we determined the location of each latex bead as one of three kinds of adherent distribution on the platelet thrombus as described in the experimental section (Fig. 4a). The average number of beads adhered for the rGPIbα-latex beads located at the front, the side, and the back of one platelet thrombus was 1.7 ± 0.5, 2.3 ± 0.4, and 1.5 ± 0.6 particles, respectively, showing that they tend to be distributed on the side (Fig. 4b). In contrast, the number of H12-latex beads on the front, the side, and the back of a thrombus was 0.9 ± 0.4, 0.6 ± 0.3, and 1.7 ± 0.6 particles, respectively, showing that they especially tend to be distributed on the back.

Discussion

In the previous studies on platelet substitutes,[1-5] although the substitutes were shown to be useful in reinforcing platelet aggregation and reducing bleeding time in vivo, they were derived from human blood. We have focused on H12, which is a synthetic oligopeptide of human fibrinogen, and conjugated it to the surface of FITC-labeled latex beads.[10] The H12-latex beads in an erythrocyte suspension adhered to the surface and accumulated in a time-dependent manner when they were allowed to flow over activated platelets immobilized on a collagen surface at a shear rate of 150s^{-1}, whereas the control latex beads did not adhere at all. The adhesion of the H12-latex beads was suppressed in the presence of free H12 as an inhibitor of GPIIb/IIIa binding,

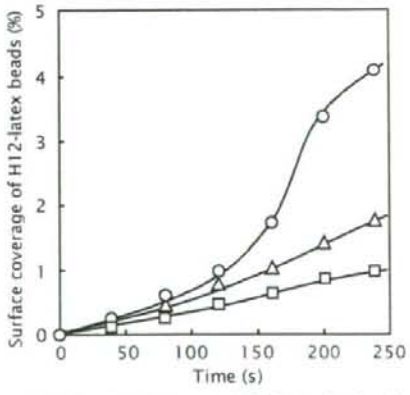

Fig. 3. Average surface coverage of H12-latex beads in thrombocytopenia-imitation blood containing (○) H12-latex beads (5.0×10^4/μl) and rGPIbα-latex beads (5.0×10^4/μl), (△) H12-latex beads (1.0×10^5/μl), and (□) control latex beads (1.0×10^5/μl) at a shear rate of 1600s^{-1}

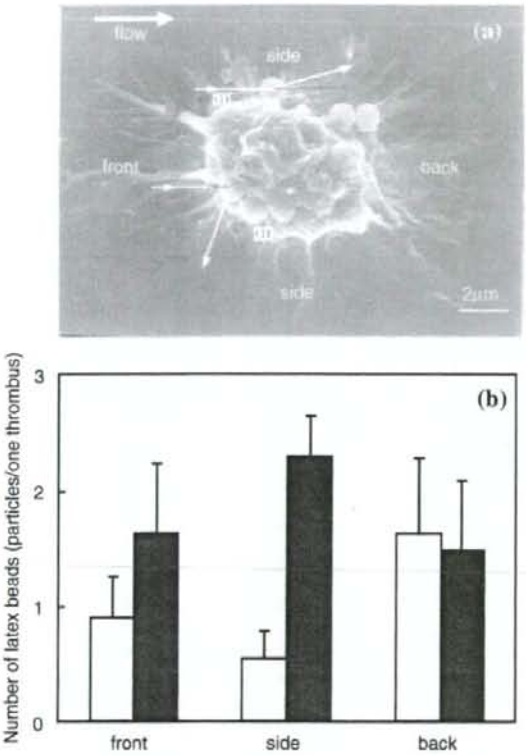

Fig. 4a. Scanning electron microscope (SEM) images of platelet thrombus formed on the collagen surface in the presence of H12-latex beads and rGPIbα-latex beads at a shear rate of $1600\,s^{-1}$. **b** Number of H12-latex beads (*open bar*) or rGPIbα-latex beads (*solid bar*) on the thrombus was estimated using the SEM after blood was passed over the collagen surface (number of thrombi: $n = 120$). *Error bars* represent SD

indicating that the adhesion was a specific interaction between the H12 and the activated GPIIb/IIIa on the immobilized platelet surface. Furthermore, the H12-latex beads showed minimal interaction with nonactivated platelets, based on the results of the flow cytometric analyses of agglutination using the FITC-labeled latex beads. Therefore, H12 is a promising candidate as a platelet substitute. However, this effect was limited to low shear rates (e.g. $150\,s^{-1}$).

Our previous studies have shown that rGPIbα-polyAlb or rGPIbα-vesicles accumulated or rolled on a VWF-immobilized surface, especially at high shear rates (e.g. $1600\,s^{-1}$).[7,10] We considered that it might be possible to combine H12 and rGPIbα as recognition sites for the purpose of constructing practical platelet substitutes which work over a wide range of shear rates.

We prepared three kinds of latex beads: H12-latex beads, rGPIbα-latex beads, and H12/rGPIbα-latex beads, the latter having both H12 and rGPIbα on the same latex bead. Latex beads were preferentially used as a model carrier because of their homogenous size and ease of detection by electron microscopic observation.

For the H12-latex beads, we conjugated H12 to the surface of the beads at a density of about $6.4 \times 10^4/\mu m^2$. This density was sufficient for the H12-conjugates to enhance the size of platelet aggregates via crosslinking between the activated GPIIb/IIIa of the platelets.[16] For the rGPIbα-latex beads, the surface density of rGPIbα, roughly $3.2 \times 10^3/\mu m^2$, was sufficient to interact with VWF immobilized on the glass surface.[10] In order to prepare H12/GPIbα-latex beads, we attempted to react SH-rGPIbα with a sufficient number of the PD groups remaining on the surface of the H12-latex beads. However, we did not obtain a GPIbα density of around $3.2 \times 10^3/\mu m^2$, but around $1.6 \times 10^3/\mu m^2$, indicating that the rGPIbα could not sufficiently bind due to steric hindrance from the H12 already bound to the latex beads. We prepared two kinds of H12/rGPIbα-latex beads, for which the density of rGPIbα was estimated to be 5.4×10^2 and $1.6 \times 10^3/\mu m^2$.

First, we confirmed the function of the H12 on the H12-latex beads and the H12/rGPIbα-latex beads using an aggregometer. ADP, which is an agonist of platelet aggregation, caused concentration-dependent platelet aggregation, resulting in the elevation of the transmittance of the platelet suspension.[28] We added ADP at a final concentration of 3μM, which caused platelet shape change and the first aggregation of platelets, but the effect was weak and did not cause the second aggregation of platelets to occur. In the case of the control albumin-adsorbed latex beads (final concentration $2.0 \times 10^3/\mu l$), the transmittance of ADP-induced platelet aggregation was 40% (Fig. 1). This value was the same as that in the absence of the latex beads (data not shown), indicating that the latex beads did not interfere with platelet aggregation. H12-latex beads significantly increased the transmittance, indicating that the H12 on the latex beads had connected to the activated GPIIb/IIIa on the ADP-stimulated platelets and cross-linked platelets; this occurred because many molecules of H12 were conjugated to each latex bead. However, the transmittance in the presence of H12/rGPIbα-latex beads was lower than the transmittance in the presence of H12-latex beads, and decreased with increasing rGPIbα conjugated on the latex bead. This suggested that the function of the H12 (Mw 1.3kDa) could be suppressed by steric hindrance from rGPIbα (Mw 50kDa) bound to the latex bead. Therefore, we concluded that the conjugation of both H12 and rGPIbα to a single latex bead was not effective and that the conjugation of H12 should employ a spacer, such as polyethylene glycol. However, this would also reduce the conjugation of rGPIbα by steric hindrance of the H12-polyethylene glycol chain.

From the above conclusion, we considered that a mixture of H12-latex beads and rGPIbα-latex beads would likely respond to a wide range of shear rates. First, we confirmed the lack of adhesion of the control latex beads to collagen at various shear rates, as shown in Fig. 2a (●), indicating that the latex beads did not interact with the collagen or activated platelets, and the surface coverage of platelets gradually decreased with the increasing shear rate [Fig. 2b (●)]. This trend is the normal behavior of the platelets flowing over a collagen surface in this condition

and the value was the same in the absence of the control (data not shown). Control latex beads did not participate in platelet adhesion and aggregation on the collagen surface.

For the H12-latex beads at a shear rate of $150 s^{-1}$, the average surface coverage increased approximately fivefold compared with the control [Fig. 2a (◊)]. The adhesion decreased considerably with increasing shear rate. This particular behavior resembles the behavior of platelets aggregated on a platelet-immobilized surface by fibrinogen crosslinking under flow.[29] We also confirmed that the fibrinogen-conjugates preferentially interacted with the platelets at low shear rates.[6]

In the same experiment, we observed platelet adhesion and confirmed that the H12-latex beads enhanced thrombus formation on the collagen surface at a shear rate of $150 s^{-1}$, and the effect gradually disappeared with increasing shear rate [Fig. 2b (◊)]. As expected from the previous report, the H12-latex beads, as a model of a platelet substitute, interacts with the activated platelets to form larger thrombi at low shear rates.

In contrast, the average surface coverage of the rGPIbα-latex beads increased with increasing shear rate [Fig. 2a (△)]; this corresponds to the well-known shear dependence of the interaction between GPIbα and VWF. Furthermore, in the presence of rGPIbα-latex beads, the platelet surface coverage tended to increase in comparison with that of the control latex beads, especially at a shear rate of $1600 s^{-1}$, indicating that the rGPIbα-latex beads also enhanced thrombus formation with the remaining platelets at high shear rates [Fig. 2b (△)]. Therefore, we confirmed that H12-latex beads alone or rGPIbα-latex beads alone were not effective in enhancement of platelet aggregation or thrombus formation over a wide range of shear rates.

We proposed the use of a mixture of the H12- and rGPIbα-latex beads to confer function over a wide range of shear rates, because the surface coverage was expected to be theoretically the arithmetic mean of both the H12-latex beads and the rGPIbα-latex beads, as shown in Fig. 2a and 2b (□). In fact, the slope of the surface coverage curve in the case of the mixed system was smaller than that for each single system, indicating that the beads in the mixed system were able to adhere over a wide range of shear rates [Fig. 2a and 2b (○)]. However, the average surface coverage tended to be higher than the arithmetic mean with increasing shear rates. If the H12-latex beads and the rGPIbα-latex beads functioned independently, the surface coverage at a shear rate of $1600 s^{-1}$ would have been the same as the arithmetic mean.

To determine the reason for the above observation, we used H12-latex beads labeled with fluorescent marker FITC and evaluated the time course of adhesion of H12-latex beads in the mixed system at a shear rate of $1600 s^{-1}$. We had determined that H12-latex beads alone could not adhere at a high shear rate [Fig. 2a (◊)]. However, the initial binding rate of the H12-latex beads in the mixed system was slow and then increased with time [Fig. 3 (○)].

To consider the above phenomena, we immunocytochemically observed platelet thrombi involving H12-latex beads or rGPIbα-latex beads after exposure to flow at a shear of $1600 s^{-1}$ using a scanning electron microscope. We visually reconfirmed that the number of rGPIbα-latex beads adhering to a thrombus was more than that of H12-latex beads, and that the H12-latex beads adhered even at high shear rates. Furthermore, the rGPIbα-latex beads tended to be located on the side of a platelet thrombus, whereas the H12-latex beads tended to be located at the back (Fig. 4). It is known that stagnation and reattachment points are generated at the downstream part (back) of stenosis in vessels.[30,31] The point of thrombus formation is usually the point of fluid stagnation, i.e., areas of low shear rates. In particular, because blood is a non-Newtonian fluid, the burble and reattachment points tend to occur in more stagnant regions. Furthermore, the fluid velocity is zero at the point of collision (front) with the stenosis. We considered that this property could be exploited for adhesion of latex beads in the process of platelet thrombus formation. The reason that H12-latex beads in the mixed system adhered to the collagen even at a shear rate of $1600 s^{-1}$ was considered to be as follows: first, rGPIbα-latex beads could adhere to the collagen surface at high shear rates, and in doing so enhance platelet thrombus formation. Second, blood fluid would tend to become stagnant at the front or back of the thrombus, and H12-latex beads could adhere to these sites even at high shear rates. At the same time, adhesion of rGPIbα-latex beads would also be enhanced at the side of the thrombus. Finally, platelet thrombus formation would be enhanced by their cooperative effects.

Conclusions

A mixture of H12-latex beads and rGPIbα-latex beads was found to have a tendency to enhance thrombus formation over a wide range of shear rates by their cooperative effects in comparison with each of the beads used alone. After further evaluating the function of the H12- or rGPIbα-latex beads in vitro, we are planning to test more biocompatible particles such as phospholipid vesicles or polymerized albumin particles for in vivo investigation. Thus, such biocompatible particles may be suitable candidates for an alternative to human platelet concentrates transfused into thrombocytopenic patients.

Acknowledgments The authors thank Drs. M. Murata and K. Yokoyama of Keio University for useful discussion about the functional evaluation of H12 peptide. This work was supported in part by Health and Labor Sciences Research Grants from the Ministry of Health, Labor and Welfare of Japan (Research on Pharmaceutical and Medical Safety, S.T., M.H., and Y.I.) and grants-in-aid from the Japan Society for the Promotion of Science (JSPS, No. 15300171, S.T.); the Ministry of Education, Culture, Sports, Science and Technology (MEXT, Leading Project for Biosimulation, M.H.); and 21COE "Practical Nano-Chemistry" and "Consolidated Research Institute for Advanced Science and Medical Care," also from MEXT (S.T.). Y.O. was the recipient of a Research Fellowship from the JSPS for Young Scientists.

References

1. Graham SS, Gonchoroff NJ, Miller JL. Infusible platelet membranes retain partial functionality of the platelet GPIb/IX/V receptor complex. Am J Clin Pathol 2001;115:144–147
2. Rybak M, Renzulli LA. A liposome-based platelet substitute, the plateletsome, with hemostatic efficacy. Biomater Artif Cells Immobil Biotechnol 1993;21:108–118
3. Agam G, Livine AA. Erythrocytes with covalently bound fibrinogen as a cellular replacement for the treatment of thrombocytopenia. Eur J Clin Invest 1992;22:105–112
4. Levi M, Friedrich PW, Middleton S, De Groot PG, Wu YP, Harris R, Biemond BJ, Heijien FG, Levin J, ten Cate JW. Fibrinogen-coated albumin microcapsules reduce bleeding in severely thrombocytopenic rabbits. Nat Med 1999;5:107–111
5. Coller BS, Springer KT, Beer JH, Mohandas N, Scudder LE, Norton KJ, West SM. Thromboerythrocytes. In vitro studies of a potential autologous, semi-artificial alternative to platelet transfusion. J Clin Invest 1992;89:546–555
6. Takeoka S, Teramura Y, Okamura Y, Handa M, Ikeda Y, Tsuchida E. Fibrinogen-conjugated albumin polymers and their interaction with platelets under flow conditions. Biomacromolecules 2001;2:1192–1197
7. Takeoka S, Teramura Y, Ohkawa H, Ikeda Y, Tsuchida E. Conjugation of von Willebrand factor-binding domain of platelet glycoprotein Ibα to size-controlled albumin microspheres. Biomacromolecules 2000;1:290–295
8. Teramura Y, Okamura Y, Takeoka S, Tsuchiyama H, Narumi H, Kainoh M, Handa M, Ikeda Y, Tsuchida E. Hemostatic effects of polymerized albumin particles bearing rGPIa/IIa in thrombocytopenic mice. Biochem Biophys Res Commun 2003;306:256–260
9. Okamura Y, Takeoka S, Teramura Y, Maruyama Y, Tsuchida E, Handa M, Ikeda Y. Hemostatic effects of fibrinogen-γ chain dodecapeptide-conjugated polymerized albumin particles in vitro and in vivo. Transfusion 2005;45:1221–1228
10. Takeoka S, Teramura Y, Okamura Y, Tsuchida E, Handa M, Ikeda Y. Rolling properties of rGPIbα-conjugated phospholipid vesicles with different membrane flexibilities on vWf surface under flow conditions. Biochem Biophys Res Commun 2002;296:765–770
11. Okamura Y, Ippei M, Teramura Y, Maruyama Y, Tsuchida E, Handa M, Ikeda Y, Takeoka S. Hemostatic effects of phospholipid vesicles carrying fibrinogen-γ chain dodecapeptide in vitro and in vivo. Bioconjug Chem 2005;16:1589–1596
12. Nishiya T, Kainoh M, Murata M, Handa M, Ikeda Y. Reconstitution of adhesive properties of human platelets in liposomes carrying both recombinant glycoproteins Ia/IIa and Ibα under flow conditions: specific synergy of receptor–ligand interactions. Blood 2002;100:136–142
13. Nishiya T, Murata M, Handa M, Ikeda Y. Targetting of liposomes carrying recombinant fragments of platelet membrane glycoprotein Ibα to immobilized von Willebrand factor under flow conditions. Biochem Biophys Res Commun 2000;270:755–760
14. Kloczewiak M, Timmons S, Hawiger J. Localization of a site interacting with human platelet receptor on carboxy-terminal segment of human fibrinogen γ chain. Biochem Biophys Res Commun 1982;107:181–187
15. Kloczewiak M, Timmons S, Lukas TJ, Hawiger J. Platelet receptor recognition site on human fibrinogen. Synthesis and structure–function relationship of peptides corresponding to the carboxy-terminal segment of the γ chain. Biochemistry 1984;23:1767–1774
16. Kloczewiak M, Timmons S, Bednarek MA, Sakon M, Hawiger J. Platelet receptor recognition domain on the γ chain of human fibrinogen and its synthetic peptide analogues. Biochemistry 1989;28:2915–2919
17. Lam SC, Plow EF, Smith MA, Andrieux A, Ryckwaert JJ, Marguerie G, Ginsberg MH. Evidence that arginyl-glycyl-aspartate peptides and γ chain peptides share a common binding site on platelets. J Biol Chem 1987;262:110–115
18. Hallahan DE, Geng L, Cmelak AJ, Chakravathy AB, Martin W, Scarfone C, Gonzalez A. Targeting drug delivery to radiation-induced neoantigens in tumor microvasculature. J Controlled Release 2001;74:183–191
19. Takeoka S, Okamura Y, Teramura Y, Watanabe N, Suziki H, Tsuchida E, Handa M, Ikeda Y. Function of fibrinogen γ-chain dodecapeptide-conjugated latex beads under flow. Biochem Biophys Res Commun 2003;312:773–779
20. Murata M, Ware J, Ruggeri ZM. Site-directed mutagenesis of a soluble recombinant fragment of platelet glycoprotein Ibα demonstrating negatively charged residues involved in von Willebrand factor binding. J Biol Chem 1991;266:15474–15480
21. Marchese P, Saldivar E, Ware J, Ruggeri ZM. Adhesive properties of the isolated amino-terminal domain of platelet glycoprotein Ibα in a flow field. Proc Natl Acad Sci USA 1999;96:7837–7842
22. Kitaguchi T, Murata M, Iijima K, Kamide K, Imagawa T, Ikeda Y. Characterization of liposomes carrying von Willebrand factor-binding domain of platelet glycoprotein Ibα: A potential substitute for platelet transfusion. Biochem Biophys Res Commun 1999;261:784–789
23. Ikeda Y, Handa M, Kawano K, Kamata T, Murata M, Araki Y, Ando H, Kawai Y, Watanabe K, Itagaki I, Sakai K, Ruggeri ZM. The role of von Willebrand factor and fibrinogen in platelet aggregation under varying shear stress. J Clin Invest 1991;87:234–1240
24. Christophor AS, Brian JL, Kandice KM, Steven JE, David LW, Roger EM. Shear-dependent changes in the three-dimensional structure of human von Willebrand factor. Blood 1996;88:2939–2950
25. Savage B, Sixma JJ, Ruggeri ZM. Functional self-association of von Willebrand factor during platelet adhesion under flow. Proc Natl Acad Sci USA 2002;99:425–430
26. Ruggeri ZM. Structure of von Willebrand factor and its function in platelet adhesion and thrombus formation. Best Prac Res Clin Haematol 2001;14:257–279
27. Suzuki H, Yamazaki H, Tanoue K. Immunocytochemical studies on co-localization of α-granule membrane $\alpha_{IIb}\beta_3$ integrin and intragranular fibrinogen of human platelets and their cell-surface expression during the thrombin-induced release reaction. J Electron Microsc 2003;52:183–195
28. Liu J, Pestina TI, Berndt MC, Steward SA, Jackson CW, Gartner TK. The role of ADP and TXA_2 in botrocetin/vWF-induced aggregation of washed platelets. J Thromb Haemost 2004;2:2213–2222
29. Bonnefoy A, Liu Q, Legrand C, Frojmovic MM. Efficiency of platelet adhesion to fibrinogen depends on both cell activation and flow. Biophys J 2000;78:2834–2843
30. Lee JS, Fung YC. Flow in nonuniform small blood vessels. Microvasc Res 1971;3:272–287
31. Forrester JH. Flow through a converging–diverging tube and its implication in occlusive vascular disease-I. J Biomech 1970;3:297–305

総　説

血小板代替物の開発の現状

Development of Platelet Substitutes

岡村陽介[1]，藤枝俊宣[1]，半田　誠[2]，池田康夫[3]，武岡真司[1]

Yosuke Okamura [1], Toshinori Fujie [1], Makoto, Handa [2], Yasuo Ikeda [3], and Shinji Takeoka [1]

和文抄録

血小板は，血液凝固系と連動した巧妙でかつ複雑な止血機構を有しており，これら全てを人工系で模倣することは不可能といっても過言ではない．我々は，血小板が出血部位を認識して粘着，凝集する分子機構に着目し，血管損傷部位や血小板表面を認識できる分子をナノ粒子の表面に担持できれば，出血部位へ特異的に集積して血栓形成を誘導する起点となり　集積したナノ粒子が出血部位を充填する効果が期待できるとの発想から，極めて単純な血小板代替物の設計に結びつけ　．具体的には，生体投与可能なリン脂質二分子膜小胞体（リポソーム）やアルブミン重合体などのナノ粒子を構築し，認識部位の候補として血小板膜糖蛋白質の一部の遺伝子組換体（rGPIbα，rGPIa/IIa）やフィブリノーゲンγ鎖C末端アミノ酸配列（HHLGGAKQAGDV: H12）をナノ粒子の表面に結合させて，in vitro，in vivoにて止血能を評価し，具体的な止血効果に関する知見が得られている．

Abstract

History of platelet substitutes is shallow with few examples of research compared with red blood cells. A platelet has complicated functions, such as tethering, rolling, adhesion, aggregation, clot retraction, and procoagulant activity. It seems to be difficult to develop platelet substitutes having all these functions. On the other hand, the basic and important functions of platelets are adhesion and aggregation in primary hemostasis. This can be easily understood from the bleeding diseases such as Bernard-Soulier syndrome or Grantzmann's thrombasthenia which lacked adhesion and condensation ability.

We considered that the hemostastic effect can be expected by infusion of nanocarriers having platelet adhesion and the aggregation ability due to the assistance of the function of the remaining platelets by infused nanocarriers. Therefore, we designed two kinds of biocompatible nanocarriers such as phospholipid vesicles and polymerized albumin particles carrying recombinant GPIbα, GPIa/IIa and fibrinogen γ-chain dodecapeptide (H12) in order to provide recognition ability for vascular injury.

K　ords

platelet substitute, phospholipid vesicles, polymerized albumin particles, rGPIbα, rGPIa IIa,, fibrinogen γ-chain dodecapeptide (H12), hemostasis

1．はじめに

医療の目覚しい進歩に伴い，癌・造血器腫瘍などの化学治療や放射線治療が年々増加する一方，その副作用によって血小板減少患者が増大しているのが現状である．血小板輸血は，化学治療や放射線治療や，外科手術において不可欠な補助治療法として非常に重要な位置を占めており，その供給量は年々増加し続け，2001年以降はほぼ横ばいとなっている[1]．しかし，血小板製剤の保存期間は日本の場合３日間と非常に短いため，供給不足に加えて緊急時の供給体制は整っていない，更には，核酸増幅検査（NAT）の導入により血液製剤の安全性は著しく向

(1) 早稲田大学大学院 理工学研究科　〒169-8555　東京都新宿区大久保3-4-1　Graduate School of Science and Engineering, Waseda University, 3-4-1 Ohkubo, Shinjuku-ku, Tokyo 169-8555, Japan.

(2) 慶応義塾大学 医学部 輸血細胞療法部　〒169-8582　東京都新宿区信濃町35　Department of Transfusion Medicine & Cell Therapy, Keio University School of Medicine, 35 Shinanomachi, Shinjuku-ku, Tokyo, 169-8582, Japan.

(3) 慶応義塾大学 医学部 内科　〒169-8582　東京都新宿区信濃町35　Department of Internal Medicine, Keio University School of Medicine, 35 Shinanomachi, Shinjuku-ku, Tokyo, 169-8582, Japan.

論文受付 2006年４月18日　論文受理 2006年４月28日

上したものの，未だにウィルス感染などのリスクは完全には取除かれてはいない．不必要な輸血を減少させる努力が払われているものの，赤血球輸血とは異なり自己血輸血の推進は図れず，同種血輸血を可及的に回避し得る血小板代替物の開発ならびに臨床応用は，21世紀に於ける医療において当然目指すべき方向であると考えられている[2]．

2．血小板の止血の機序と血小板代替物の設計

止血の重要な初期段階は，血管損傷部位に露出した血管内皮下組織，特にコラーゲンへの血小板の粘着と凝集である．血小板の膜表面には，コラーゲンやそれに結合したフォンビレブランド因子（VWF）を認識する受容体があり，これらの相互作用により接着や粘着が起こる．高血流条件下では，血小板膜糖蛋白質Ib（GPIb）がVWFを介したコラーゲンとの相互作用によって血小板の接着（ローリング）が起こり，ローリング速度を緩やかになる[3]．次いで，コラーゲン受容体であるGPIa/IIa（$\alpha_2\beta_1$インテグリン）やGPVIがコラーゲンと直接結合してより強固に粘着する[4,5]．更には，接着，粘着の刺激が細胞内に伝わり，複雑なシグナル伝達経路を経て血小板膜糖蛋白質GPIIb/IIIa（$\alpha_{IIb}\beta_3$インテグリン）が“折れ曲がり状態”から“立上がり状態”へと高次構造が変化し（活性化），血漿蛋白質であるフィブリノーゲンやVWFを介した血小板凝集（一次凝集）が起こる[6]．同時に，細胞内シグナル伝達によって血小板の形態が変化して偽足を出して伸展し，血小板内の濃染顆粒が解放小管系の膜と融合して血小板活性化因子であるCa^{2+}，セロトニン，アデノシン5'-二リン酸（ADP）が放出され，ポジティブフィードバックによって更に血小板の活性化が亢進する．次に，α顆粒からフィブリノーゲン，VWF，P-セレクチン，フィブロネクチンなどを放出，同時にこれらの受容体を血小板表面に発現し，血小板間，あるいは白血球をも巻き込んだネットワークを形成して血小板凝集（二次凝集，ここまで一次止血と呼ぶ）を促す[7]．最後に強力な凝固系因子であるトロンボキサンA_2の放出や血小板表面が凝固系の活性に必要な場（ホスファチジルセリン）が提供され，血漿中の凝固系が活性化されて最終的にはフィブリノーゲンがフィブリン塊（血餅）となって止血（二次止血）が完了する．

このように血小板による止血は，血小板の粘着，凝集，変形や顆粒の放出など，非常に巧妙かつ複雑に制御された多段階の反応が動的に連動しているため，この機能を全て模倣した人工系の構築は不可能と言ってよい．そこで，著者らは，血小板が出血部位を認識して粘着，凝集する分子機序に着目し，血管損傷部位や血小板表面を認識できる分子をナノ粒子表面に担持できれば，出血部位へ特異的に集積して血栓形成を誘導する起点となり，集積したナノ粒子が出血部位を充填する効果が期待できるとの発想から，極めて単純な血小板代替物の設計から検討を開始した（Fig. 1.）．

3．海外の血小板代替物の開発動向

血小板代替物の研究は，フィブリノーゲンを吸着させたラテックスビーズがADP刺激による活性化血小板と迅速に反応することをColler ら[8]が1980年に報告したことに始まる．その後，担体として正常ヒト赤血球にフィブリノーゲン[9]やその一部のアミノ酸配列RGD[10]を固相化した例が報告され，血小板の凝集反応を媒介するリガンドの固相化により残存血小板の凝集能を増強する実例となった．1999年にはLeviら[11]により，フィブリノーゲンを吸着させた粒子径が約3 μmのアルブミンマイクロカプセルを調製し，血小板減少ラビットへ投与した出血時間の短縮が詳細に報告された．他方，ヒト血小板を凍結融解にて破壊後加熱処理した粉末製剤（Infusible Platelet Membrane）が血小板減少ラビットの出血時間を短縮した例[12]が報告され臨床試験が開始されたものの，作用機序が不明瞭であることなどがの理由により，臨床試験は中断されている．しかし，上述の例は，全てヒト血液由来の成分を使用しており，ウイルス感染の危険性は否めない．

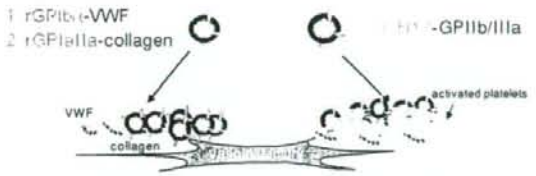

Fig. 1. Design of Platelet substitutes.

我が国における血小板代替物の開発は，生体投与可能なリン脂質小胞体（リポソーム）や遺伝子組換えヒト血清アルブミン（rHSA）の重合体をナノ粒子として利用し，血小板の止血に関する分子機序を利用して，出血部位を認識させるために血小板膜糖蛋白質の一部の遺伝子組換え体（rGPIbα，rGPIa/IIa）やフィブリノーゲンγ鎖C末端アミノ酸配列（HHLGGAKQAGDV: H12）を担持させて，血小板を巻き込んだ出血部位への集積により止血能の発現を期待している．

4．ナノ粒子の調製方法

リン脂質を水中に分散させると自発的に集合し，多重層の二分子膜小胞体（リポソーム）が構築される[13]．これを孔径の異なるフィルターに順次透過させると，粒子径と層数の制御と同時に様々な水溶性物質を内包できる（エクストルージョン法）．また，小胞体を形成させてから表面に認識部位を担持させることもできる（Fig. 2. (a)）．一般に小胞体には次の長所が挙げられる．①膜成分であるリン脂質やコレステロールは生体適合性，生分解性に優れる，②水溶性や脂溶性の低分子薬物，蛋白質や遺伝子などの高分子を封入できる，③粒径や脂質組成により血中滞留時間や体内動態を調節できる[14]，④小胞体の表面へ多くの蛋白質を担持させて特定部位への指向性，集積性（ターゲティング）が期待できる[15-17]．小胞体の内水相に高濃度ヘモグロビン（Hb）を内包させて，その表面をポリエチレングリコール修飾した酸素運搬体は，高い酸素運搬効果と長い血中滞留性や保存安定性を持ち[18]，霊長類や中動物を用いてその効果と安

全性の確認が進んでいる．

他方，ヒト血清アルブミンは，5g/dLと血漿蛋白質の中で最も多い蛋白質であり，コロイド浸透圧の調節や，栄養物や代謝物などの運搬を担っている．これを利用した微粒子（例えば，アルブミン大凝集体，アルブミンマイクロスフェア，アルブミンマイクロカプセルなど）は生体適合性・生分解性を有するため，既に1950年代から静注用製剤として血管造影剤，超音波診断用増感剤や徐放性薬物担体などに臨床使用されている．しかしながら，これらのアルブミン粒子は，高温加熱処理（スプレードライ法）や有機溶媒による不可逆な変性や界面活性剤や架橋剤を用いるため，粒子径の制御や添加物の除去操作が煩雑であった[19]．そこで我々は，①遺伝子組換えヒト血清アルブミン（rHSA）[20]をビルディングブロックとしてrHSAをジスルフィド結合にて重合する方法を用いて，②重合度の制御によりナノからマイクロスケールの粒径制御を可能とし，③水溶液中でのp[illegible]温度の制御にて重合するクリーンな方法を採用して，親水性の表面を持つ粒子を調製でき，④アルブミン変性がほとんどない重合体を得る方法を確立している[21]．アルブミン重合体は内部が充填された無定形な"ぼたん雪"のような形態をとっており，例えば出血部位での充填効果が期待できる（Fig. 2. (b)）．

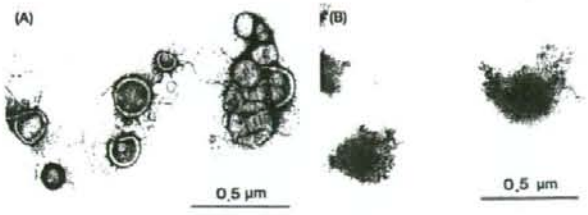

Fig. 2. TEM images of (A) phospholipid vesicles and (B) polymerized albumin particles.

5．血小板代替物の機能評価

小胞体の表面にrGPIbα[22]を結合させると血小板の接着現象（[illegible]・リング）が再現できる．高血流条件下での血小板による止血は，血小板表面のGPIbαがコラーゲンに結合したVWFを認識して血小板が接着することから始まる．抗GPIIb/IIIa抗体を添加した血小板をフローチャンバーに設置し流動下での*in vitro*観測を行うと，VWF固定化基板上を流動方向に沿ってローリングする現象が観察される．rGPIbαを結合させた小胞体でも同様にVWF基板上をローリングすることが確認された（Fig. 3. (a)）[23]．興味深いことに，そのローリング速度は，小胞体を構成するリン脂質二分子膜の柔軟性（membrane flexibility）と相関していることが明らかになった[23]．即ち，粒子径やrGPIbαの表面結合密度を統一して柔軟性のみの異なる小胞体を用いて比較したところ，"柔らかい"小胞体ではローリング速度は低下し，"硬い"小胞体では上昇した．これは"柔らかい"小胞体は変形しやすくVWF基板と小胞体間の接触面積が増大したためにローリング速度が低下したためと考えられる．ところが，アルブミン重合体ではVWF表面をローリングせずに直ちに粘着して停止する（Fig. 3. (b)）．同様の挙動は，ラテックスビーズや固定化血小板でも認められたことから，ローリングの性質を持たせるには流動性のある膜構造を持つことが必要条件であることが明らかになった．

rGPIa/IIaを結合させた小胞体では，低血流条件下でコラーゲン基板を特異的に認識して粘着する挙動が西谷らによって報告された[24]．血流速度の増大と共にコラーゲン基板への粘着数は減少するが，一つの小胞体にrGPIbαとrGPIa/IIaの両者を担持させると低血流速度から高血流速度の範囲にわたってコラーゲン基板に粘着する微粒子となる[25]．我々は，rGPIa/IIa担持アルブミン重合体でも同様の性質を確認した．これをX線照射にて血小板数を正常値の5分の1程度に減少させたマウスに投与して尾先端を切断して出血時間の測定を行ったところ，コントロール群の出血時間（730±198秒）と比較して投与量依存的に出血時間の短縮が認められた（例えば，2.4×10^{11} particles/kgでは出血時間は337±46秒）（Fig. 4.）[26]．

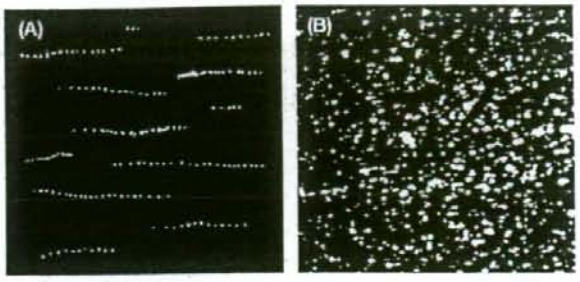

Fig. 3. Specific interaction of (A) phospholipid vesicles carrying rGPIbα and (B) polymerized albumin particles carrying rGPIbα with VWF-immobilized surface at the shear rate of 2400 s^{-1}. (A) and (B) were superimposed of pictures for 3 s taken at every 1/6 s.

さらに，粘着して活性化した血小板同士を架橋するフィブリノーゲンを結合させた微粒子は減少した残存血小板の凝集補助として期待できる[27]．実際，血小板数が正常値の5分の1程度に調節された血小板減少モデル血液にフィブリノーゲンを結合させたアルブミン重合体を添加すると，添加量の増大と共に流動血小板の粘着数が増大したことから，フィブリノーゲン結合アルブミン重合体は血小板凝集増強効果を有する微粒子であることが示唆された．しかし，フィブリノーゲンは4℃で保存すると凝集する非常に扱いにくい蛋白質であり[28]，水溶液中では速やかに失活することも判明した[27]．

そこで，活性化血小板膜上のGPIIb/IIIaを認識サイトとして知られているフィブリノーゲンのγ鎖C末端の400-411番目のドデカペプチド（HHLGGAKQAGDV，H12）とα鎖の95-98あるいは572-575番目のテトラペプチド（RGDS，RGDF）を血小板代替物の認識部位として着目し，担体にラテックスビーズを用いて両者の機能比較を行った[29]．正常血小板（2.0×10^{4} /μL）に対するラテックスビーズ，H12あるいはRGDを結合させたラテックスビーズ（1.0×10^{5} /μL）の非特異的粘着率をフローサイトメトリーにて算出した（Fig. 5.），H12結合ラテックスビーズ

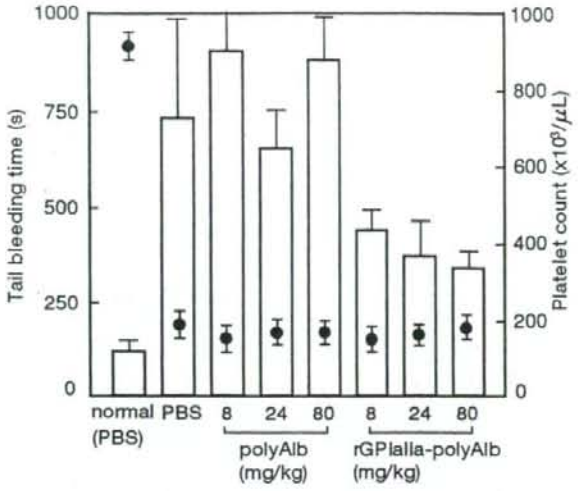

Fig. 4. Effect of the administration of polymerized albumin particles carrying rGPIa/IIa on the tail bleeding time (white columns). The administered amounts of polymerized albumin particles carrying rGPIa/IIa are 8, 24, and 80 mg/kg. Circles show platelet counts in the mouse.

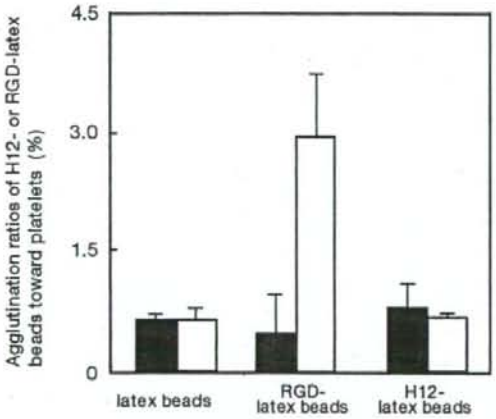

Fig. 5. Agglutination ratios of H12- or RGD-conjugated latex beads toward platelets by flow cytometry. 0 min (filled columns) and 30 min (open columns), after mixing with H12- or RGD-latex beads and platelets.

では，正常血小板に対する非特異的粘着率に変化はみられず，血小板とほとんど相互作用しないと考えられた．他方，RGD結合ラテックスビーズでは血小板に対する非特異的粘着率が2.9±1.3 %まで上昇した（Fig. 5.）．このことから，RGD結合ラテックスビーズは正常血小板と相互作用して，血流中で血栓形成を引き起こす可能性が示唆された．さらに，H12結合ラテックスビーズと正常血小板を混合した後も血小板の活性化を引起さないことを証明した．具体的には，血小板の活性化マーカーであるGPIIb/IIIa やP-セレクチンの発現を，それぞれの抗体であるPAC-1と抗P-セレクチン抗体にて解析した[20]．例えば，Table 1. に示すように，ADP刺激した血小板はPAC-1陽性率が55.1±6.1 %であり，未刺激（PBS群）の血小板のそれ（0.4±0.1 %）と比較すると明らかにGPIIb/IIIaの活性化を認める．同様にADP刺激した血小板では，P-セレクチンの発現率も著しく上昇し31.6±6.9 %と非常に高くなっている．しかしながら，H12結合ラテックスビーズと混合した血小板では，GPIIb/IIIaあるいはP-セレクチンの発現はいずれも認められず，PBS群とほとんど差はみられなかった．このことから，H12結合ラテックスビーズは正常血小板を活性化することなく，血小板に対して不活性であることを証明した．

次いで，血小板減少モデル血液中（2.0x10⁴ /μL，正常の10

Table 1. PAC-1 binding and P-selectin expression to platelets in the presence of H12-conjugated latex beads.

	PAC-1 binding (%)		P-selectin expression (%)	
Stirring time (min)	0	10	0	10
PBS	0.43±0.12	1.75±0.41	0.50±0.01	0.70±0.14
H12-latex beads	0.47±0.20	1.49±0.26	0.53±0.04	0.75±0.23
Positive control	55.1±6.1 [1]		31.6±6.9 [2]	

1) ADP 100 μM, 2) ADP 20 μM

分の1）にH12結合ラテックスビーズを添加し，コラーゲン基板に対する血小板の粘着挙動を観察したところ，H12結合ラテックスビーズの未添加系と比較して血小板の粘着面積を約2倍も増大させた．さらに，血液流動後の基板を走査電顕観察したところ，コラーゲン基板上にまず血小板が粘着した後にH12結合ラテックスビーズが結合し，さらにこれを巻き込むようにして血小板が凝集している様子が確認できた（Fig. 6.）．これは，H12結合ラテックスビーズが，血小板凝集を促進していることを支持する結果である．

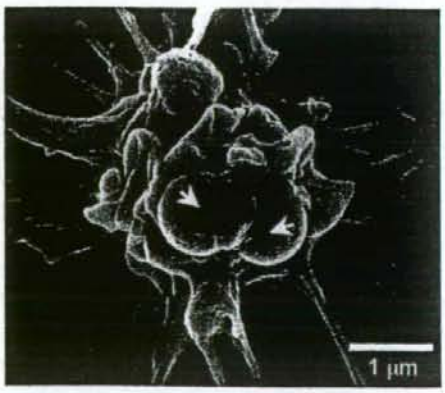

Fig. 6. SEM image obtained after platelets mixed with H12-latex beads were passed over collagen immobilized on a glass surface. Arrows in the SEM image are H12-latex beads.